

# Control Barriers in Bayesian Learning of System Dynamics

Vikas Dhiman\* Mohammad Javad Khojasteh\* Massimo Franceschetti Nikolay Atanasov

**Abstract**—This paper focuses on learning a model of system dynamics online while satisfying safety constraints. Our objective is to avoid offline system identification or hand-specified models and allow a system to safely and autonomously estimate and adapt its own model during operation. Given streaming observations of the system state, we use Bayesian learning to obtain a distribution over the system dynamics. Specifically, we use a matrix variate Gaussian process (MVGP) regression approach with efficient covariance factorization to learn the drift and input gain terms of a nonlinear control-affine system. The MVGP distribution is then used to optimize the system behavior and ensure safety with high probability, by specifying control Lyapunov function (CLF) and control barrier function (CBF) chance constraints. We show that a safe control policy can be synthesized for systems with arbitrary relative degree and probabilistic CLF-CBF constraints by solving a second order cone program (SOCP). Finally, we extend our design to a self-triggering formulation, adaptively determining the time at which a new control input needs to be applied in order to guarantee safety.

**Index Terms**—Gaussian Process, learning for dynamics and control, high relative-degree system safety, control barrier function, self-triggered safe control

## SUPPLEMENTARY MATERIAL

Software and videos supplementing this paper are available at: [https://vikasdhiman.info/Bayesian\\_CBF](https://vikasdhiman.info/Bayesian_CBF)

## I. INTRODUCTION

Unmanned vehicles and other cyber-physical systems [2], [3] promise to transform many aspects of our lives, including transportation, agriculture, mining, and construction. Successful use of autonomous systems in these areas critically depends on safe adaptation in changing operational conditions. Existing systems, however, rely on brittle hand-designed dynamics models and safety rules that often fail to account for both the complexity and uncertainty of real-world operation. Recent work [4]–[19] has demonstrated that learning-based system identification and control techniques may be successful at complex tasks and control objectives. However, two critical considerations for applying these techniques onboard autonomous systems remain less explored: *learning* online, relying on streaming data, and guaranteeing *safe* operation, despite the estimation errors inherent to learning algorithms.

\* The first two authors contributed equally.

The material in this paper was presented in part at the 2020 Learning for Dynamics and Control Conference (L4DC) [1]. We gratefully acknowledge support from ARL DCIST CRA W911NF-17-2-0181 and NSF awards CNS-1446891, ECCS-1917177, and IIS-2007141.

V. Dhiman, M. Franceschetti, and N. Atanasov are with Department of Electrical and Computer Engineering, University of California San Diego, La Jolla, CA 92093. (e-mails: {vdhiman, mfranceschetti, natanasov}@ucsd.edu)

M. J. Khojasteh is with Massachusetts Institute of Technology, Cambridge, MA 02139. This work was performed while at California Institute of Technology and University of California, San Diego. (e-mail: mkhojast@mit.edu)

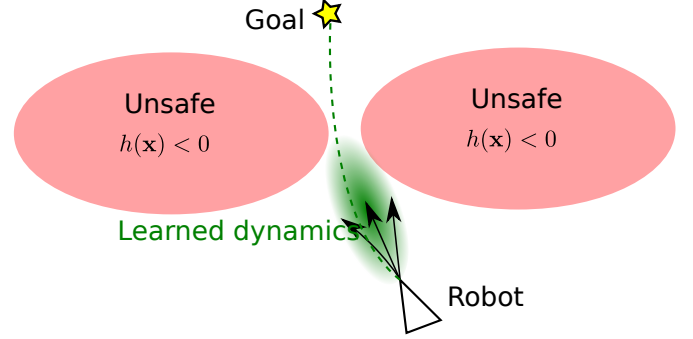


Fig. 1. A motivating example: consider steering a Ackermann-drive vehicle, whose dynamics are not perfectly known, safely to a goal location. We develop a matrix variate Gaussian process regression method to estimate the system dynamics online and show how the probability distribution of the dynamics affects optimization-based control synthesis with control Lyapunov and control barrier constraints. Our simulations show that the proposed controller navigates through the obstacles only when the variance of the estimated dynamics is sufficiently small.

For example, consider steering a Ackermann-drive vehicle, whose dynamics are not perfectly known, safely to a goal location (Fig. 1). Not only does the Ackermann vehicle need to *learn* a distribution over its dynamics from state and control observations but also account for the variance of the dynamics to *guarantee safety* while executing its actions.

Several approaches have been proposed in the literature to guarantee safety of dynamical systems. Motivated by the utility of Lyapunov functions for certifying stability properties, [20]–[29] proposed *control barrier functions* (CBFs) as a tool to enforce safety properties in dynamical systems. A CBF certifies whether a control policy achieves forward invariance of a *safe set*  $\mathcal{C}$  by evaluating if the system trajectory remains away from the boundary of  $\mathcal{C}$ . A lot of the literature on CBFs considers systems with known dynamics, low relative degree, no disturbances, and time-triggered control, in which inputs are recalculated at a fixed and sufficiently small period. Time-triggered control is limiting because low frequency may lead to safety violations in-between sampling times, while high frequency leads to inefficient use of computational resources and actuators. Yang et al. [30] extend the CBF framework, for *known dynamics*, to an event-triggered setup [31]–[34] in which the longest time until a control input needs to be recomputed to guarantee safety is provided. CBF techniques can handle nonlinear control-affine systems but many existing results apply only to relative-degree-one systems, in which the first time derivative of the CBF depends on the control input. This requirement is violated by many underactuated robot systems and motivates extensions to relative-degree-two systems, such as bipedal and car-like robots. The works [35]–[38] generalized these ideas, in the case of *known dynamics*,

by designing exponential control barrier function (ECBF) and high order control barrier function (HOCBF), that can handle control-affine systems with any relative degree.

Our work proposes a Bayesian learning approach for estimating the posterior distribution of the control-affine system dynamics from online data. We generalize the CBF control synthesis techniques to handle probabilistic safety constraints induced by the dynamics distribution. Our work makes the following **contributions**. First, we develop a Matrix Variate Gaussian Process (MVGp) regression to estimate the unknown system dynamics and formulate probabilistic safety and stability constraints for systems with arbitrary relative degree. Second, we show that a control policy satisfying the proposed probabilistic constraints can be obtained as the solution of a deterministic second order cone program (SOCP). The SOCP formulation depends on the mean and variance of the probabilistic safety and stability constraints, which can be obtained efficiently. Third, we extend our results to a self-triggered safe control setting, adaptively determining the duration of each control input before re-computation is necessary to guarantee safety with high probability. Finally, we derive closed-form expressions for the mean and variance of the probabilistic safety and stability constraints, up to relative-degree two. This work extends our conference paper [1] by introducing a SOCP control-synthesis formulation instead of the original, possibly non-convex, quadratic program (QP) problem. This paper also extends the self-triggered control design to systems with relative degree above one, contains a complete technical treatment of the result—including the proofs of that were omitted in the conference version, and presents new evaluation results.

## II. RELATED WORK

Providing safety guarantees for learning-based control techniques has received significant attention recently [39]–[46]. In particular, optimization-based control synthesis with CLF and CBF constraints has been considered for systems subject to additive stochastic disturbances [47]–[49]. Aloysius Pereira et al. [49] combine CBF constraints and forward-backward stochastic differential equations, to find a deep parameterized safe optimal control policy in the presence of additive Brownian motion in the system dynamics. CBF conditions for systems with uncertain dynamics have been proposed in [50]–[57]. Fan et al. [50] study time-triggered CBF-based control synthesis for control-affine systems with relative degree one, where the input gain is known and invertible but the drift term is learned via Bayesian techniques. The authors compare the performance of Gaussian process (GP) regression [58], dropout neural networks [59], and ALPaCA [60] in constructing adaptive CLF and CBF conditions using bounds on the error with respect to a system reference model. The works in [51], [52], [54], [55] study time-triggered CBF-based control of relative-degree-one systems with additive uncertainties in the drift part of the dynamics. Wang et al. [51] use GP regression to approximate the unknown part of the 3D nonlinear dynamics of a quadrotor robot. Cheng et al. [52] propose a two-layers control policy design that integrates CBF-based control with model-free reinforcement learning (RL).

Safety is ensured by bounding the worst-case deviation of the dynamics estimate from the mean, using high-confidence polytopic uncertainty bounds. Marvi and Kiumarsi [53] also consider safe model-free reinforcement learning but, instead of a two-layer policy design, the cost-to-go function is augmented with a CBF term. The works [54], [55] use adaptive CBFs to deal with parameter uncertainty. Salehi et al. [56] employ Extreme Learning Machines to approximate the dynamics of a closed-loop nonlinear system (with a drift term only) subject to a barrier certificate constraint during the learning process itself.

Our work builds upon the current literature by developing a matrix variate GP regression with efficient covariance factorization to learn both the *drift term* and the *input gain* terms of a nonlinear control-affine system. The posterior distribution is used to ensure safety for systems with *arbitrary relative degree*. Compared to previous works, our safety constraints are less conservative (probabilistic instead of worst-case) and lead to a novel SOCP formulation. We also present results for a *self-triggering design* with unknown system dynamics.

Research directions left open for future investigation include the extension of the results to a frequentist setting [61]. Following [62], where the unknown but deterministic dynamics are assumed to belong to the Reproducing Kernel Hilbert Space (RKHS), our CBF-based self-triggered controller may be redesigned in a frequentist framework. In fact, a time-triggered setup that utilizes independent GP regression for each coordinate has been recently developed in [63], where a systematic approach is utilized to compute CBFs for the learned model.

## III. PROBLEM STATEMENT

Consider a control-affine nonlinear system:

$$\dot{\mathbf{x}} = f(\mathbf{x}) + g(\mathbf{x})\mathbf{u} = \begin{bmatrix} f(\mathbf{x}) & g(\mathbf{x}) \end{bmatrix} \begin{bmatrix} 1 \\ \mathbf{u} \end{bmatrix} \triangleq F(\mathbf{x})\underline{\mathbf{u}}, \quad (1)$$

where  $\mathbf{x}(t) \in \mathcal{X} \subset \mathbb{R}^n$  and  $\mathbf{u}(t) \in \mathcal{U} \subset \mathbb{R}^m$  are the system state and control input, respectively, at time  $t$ . Assume that the *drift term*  $f : \mathbb{R}^n \rightarrow \mathbb{R}^n$  and the *input gain*  $g : \mathbb{R}^n \rightarrow \mathbb{R}^{n \times m}$  are locally Lipschitz and the admissible control set  $\mathcal{U}$  is convex. We study the problem of enforcing stability and safety properties for (1) when  $f$  and  $g$  are unknown and need to be estimated online, using observations of  $\mathbf{x}$ ,  $\mathbf{u}$ ,  $\dot{\mathbf{x}}$ .

### A. Notation

We use bold lower-case letters for vectors ( $\mathbf{x}$ ), bold capital letters for matrices ( $\mathbf{X}$ ), and caligraphic capital letters for sets ( $\mathcal{X}$ ). The boundary of a set  $\mathcal{X}$  is denoted by  $\partial\mathcal{X}$ . Let  $\text{vec}(\mathbf{X}) \in \mathbb{R}^{nm}$  be the vectorization of  $\mathbf{X} \in \mathbb{R}^{n \times m}$ , obtained by stacking the columns of  $\mathbf{X}$ . The Kronecker product is denoted by  $\otimes$ . The Hessian and Jacobian of functions  $h : \mathbb{R}^n \times \mathbb{R}^m \rightarrow \mathbb{R}$  and  $f : \mathbb{R}^n \rightarrow \mathbb{R}^n$ , respectively, are defined as:

$$\mathcal{H}_{\mathbf{x}, \mathbf{y}} h(\mathbf{x}, \mathbf{y}) \triangleq \begin{bmatrix} \frac{\partial^2 h}{\partial x_1 \partial y_1} & \cdots & \frac{\partial^2 h}{\partial x_1 \partial y_m} \\ \vdots & & \vdots \\ \frac{\partial^2 h}{\partial x_n \partial y_1} & \cdots & \frac{\partial^2 h}{\partial x_n \partial y_m} \end{bmatrix} \quad \mathcal{J}_{\mathbf{x}} f(\mathbf{x}) \triangleq \begin{bmatrix} \frac{\partial f_1}{\partial x_1} & \cdots & \frac{\partial f_1}{\partial x_n} \\ \vdots & & \vdots \\ \frac{\partial f_n}{\partial x_1} & \cdots & \frac{\partial f_n}{\partial x_n} \end{bmatrix}.$$

The Lie derivative of  $V : \mathbb{R}^n \rightarrow \mathbb{R}$  along  $f : \mathbb{R}^n \rightarrow \mathbb{R}^n$  is denoted by  $\mathcal{L}_f V : \mathbb{R}^n \rightarrow \mathbb{R}$ . The space of  $r$  times continuously differentiable functions  $h : \mathcal{X} \rightarrow \mathbb{R}$  is denoted by  $\mathbb{C}^r(\mathcal{X}, \mathbb{R})$ .

## B. Stability and Safety with Known Dynamics

We first review key results [25] on control Lyapunov functions for enforcing stability and control barrier functions for enforcing safety of control-affine systems with *known dynamics*. System stability may be asserted as follows.

**Definition 1.** A function  $V \in \mathbb{C}^1(\mathcal{X}, \mathbb{R})$  is a *control Lyapunov function* (CLF) for the system in (1) if it is positive definite,  $V(\mathbf{x}) > 0$ ,  $\forall \mathbf{x} \in \mathcal{X} \setminus \{0\}$ ,  $V(0) = 0$ , and satisfies:

$$\inf_{\mathbf{u} \in \mathcal{U}} \text{CLC}(\mathbf{x}, \mathbf{u}) \leq 0, \quad \forall \mathbf{x} \in \mathcal{X}, \quad (2)$$

where  $\text{CLC}(\mathbf{x}, \mathbf{u}) \triangleq \mathcal{L}_f V(\mathbf{x}) + \mathcal{L}_g V(\mathbf{x})\mathbf{u} + \gamma(V(\mathbf{x}))$  is a *control Lyapunov condition* (CLC) defined for some class  $K$  function  $\gamma$ .

**Proposition 1** (Sufficient Condition for Stability [25]). *If there exists a CLF  $V(\mathbf{x})$  for system (1), then any Lipschitz continuous control policy  $\pi(\mathbf{x}) \in \{\mathbf{u} \in \mathcal{U} \mid \text{CLC}(\mathbf{x}, \mathbf{u}) \leq 0\}$  asymptotically stabilizes the system.*

Let  $\mathcal{C} \triangleq \{\mathbf{x} \in \mathcal{X} \mid h(\mathbf{x}) \geq 0\}$  be a *safe set* of system states, defined implicitly by a function  $h \in \mathbb{C}^1(\mathcal{X}, \mathbb{R})$ . System (1) is *safe* with respect to  $\mathcal{C}$  if  $\mathcal{C}$  is *forward invariant*, i.e., for any  $\mathbf{x}(0) \in \mathcal{C}$ ,  $\mathbf{x}(t)$  remains in  $\mathcal{C}$  for all  $t \geq 0$ . System safety may be asserted as follows.

**Definition 2.** A function  $h \in \mathbb{C}^1(\mathcal{X}, \mathbb{R})$  is a *control barrier function* (CBF) for the system in (1) if

$$\sup_{\mathbf{u} \in \mathcal{U}} \text{CBC}(\mathbf{x}, \mathbf{u}) \geq 0, \quad \forall \mathbf{x} \in \mathcal{X}, \quad (3)$$

where  $\text{CBC}(\mathbf{x}, \mathbf{u}) \triangleq \mathcal{L}_f h(\mathbf{x}) + \mathcal{L}_g h(\mathbf{x})\mathbf{u} + \alpha(h(\mathbf{x}))$  is a *control barrier condition* (CBC) defined for some extended class  $K_\infty$  function  $\alpha$ .

**Proposition 2** (Sufficient Condition for Safety [25]). *Consider a set  $\mathcal{C}$  defined implicitly by  $h \in \mathbb{C}^1(\mathcal{X}, \mathbb{R})$ . If  $h$  is a CBF and  $\nabla h(\mathbf{x}) \neq 0$  for all  $\mathbf{x}$  when  $h(\mathbf{x}) = 0$ , then any Lipschitz continuous control policy  $\pi(\mathbf{x}) \in \{\mathbf{u} \in \mathcal{U} \mid \text{CBC}(\mathbf{x}, \mathbf{u}) \geq 0\}$  renders the system in (1) safe with respect to  $\mathcal{C}$ .*

Note that the conditions for stability and safety are defined by affine constraints in  $\mathbf{u}$ . This observation allows the formulation of control synthesis as a quadratic program (QP) in which stability and safety properties are captured by the linear CLC and CBC constraints, respectively:

$$\begin{aligned} \pi(\mathbf{x}) \in \arg \min_{\mathbf{u} \in \mathcal{U}, \delta \in \mathbb{R}} \quad & \|\mathbf{R}(\mathbf{x})\mathbf{u}\|^2 + \lambda\delta^2 \\ \text{s.t.} \quad & \text{CLC}(\mathbf{x}, \mathbf{u}) \leq \delta, \text{CBC}(\mathbf{x}, \mathbf{u}) \geq 0, \end{aligned} \quad (4)$$

where  $\mathbf{R}(\mathbf{x}) \in \mathbb{R}^{m \times m}$  is a matrix penalizing control effort and  $\delta$  is a slack variable that ensures feasibility of the QP by giving preference to safety over stability, controlled by the scaling factor  $\lambda > 0$ . If a stabilizing control policy  $\hat{\pi}(\mathbf{x})$  is already available, it may be modified minimally online to ensure safety:

$$\begin{aligned} \pi(\mathbf{x}) \in \arg \min_{\mathbf{u} \in \mathcal{U}} \quad & \|\mathbf{R}(\mathbf{x})(\mathbf{u} - \hat{\pi}(\mathbf{x}))\|^2 \\ \text{s.t.} \quad & \text{CBC}(\mathbf{x}, \mathbf{u}) \geq 0. \end{aligned} \quad (5)$$

In practice, the QPs above cannot be solved infinitely fast. Optimization is typically performed at triggering times  $t_k, t_{k+1}, \dots$ , providing control input  $\mathbf{u}_k \triangleq \pi(\mathbf{x}_k)$  when the system state is  $\mathbf{x}_k \triangleq \mathbf{x}(t_k)$ . Ames et al. [21, Thm. 3] show that if  $f$ ,  $g$ , and  $\alpha \circ h$  are locally Lipschitz, then  $\pi(\mathbf{x})$  and  $\text{CBC}(\mathbf{x}, \pi(\mathbf{x}))$  are locally Lipschitz. Thus, for sufficiently small inter-triggering times  $\tau_k \triangleq t_{k+1} - t_k$ , solving (5) at  $\{t_k\}_{k \in \mathbb{N}}$  ensures safety during the inter-triggering intervals  $[t_k, t_{k+1})$  as well.

## C. Stability and Safety with Unknown Dynamics

This work considers stability and safety for the control-affine nonlinear system in (1) when the system dynamics  $F(\mathbf{x}) \in \mathbb{R}^{n \times (1+m)}$  are *unknown*. We place a prior distribution over  $\text{vec}(F(\mathbf{x}))$  using a GP [58] with mean function  $\text{vec}(\mathbf{M}_0(\mathbf{x}))$  and covariance function  $\mathbf{K}_0(\mathbf{x}, \mathbf{x}')$ . Our objective is to compute the posterior distribution of  $\text{vec}(F(\mathbf{x}))$  using observations of the system states and controls over time and ensure stability and safety using the estimated dynamics model despite possible estimation errors.

**Problem 1.** Given a prior distribution on the unknown system dynamics,  $\text{vec}(F(\mathbf{x})) \sim \mathcal{GP}(\text{vec}(\mathbf{M}_0(\mathbf{x})), \mathbf{K}_0(\mathbf{x}, \mathbf{x}'))$ , and a training set,  $\mathbf{X}_{1:k} \triangleq [\mathbf{x}(t_1), \dots, \mathbf{x}(t_k)]$ ,  $\mathbf{U}_{1:k} \triangleq [\mathbf{u}(t_1), \dots, \mathbf{u}(t_k)]$ ,  $\dot{\mathbf{X}}_{1:k} = [\dot{\mathbf{x}}(t_1), \dots, \dot{\mathbf{x}}(t_k)]^1$ , compute the posterior distribution  $\mathcal{GP}(\text{vec}(\mathbf{M}_k(\mathbf{x})), \mathbf{K}_k(\mathbf{x}, \mathbf{x}'))$  of  $\text{vec}(F(\mathbf{x}))$  conditioned on  $(\mathbf{X}_{1:k}, \mathbf{U}_{1:k}, \dot{\mathbf{X}}_{1:k})$ .

**Problem 2.** Given a safe set  $\mathcal{C} \triangleq \{\mathbf{x} \in \mathcal{X} \mid h(\mathbf{x}) \geq 0\}$ , initial state  $\mathbf{x}_k \triangleq \mathbf{x}(t_k) \in \mathcal{C}$ , and the distribution  $\mathcal{GP}(\text{vec}(\mathbf{M}_k(\mathbf{x})), \mathbf{K}_k(\mathbf{x}, \mathbf{x}'))$  of  $\text{vec}(F(\mathbf{x}))$  at time  $t_k$ , choose a control input  $\mathbf{u}_k$  and triggering period  $\tau_k$  such that for  $\mathbf{u}(t) \triangleq \mathbf{u}_k$ :

$$\mathbb{P}(\text{CBC}(\mathbf{x}(t), \mathbf{u}_k) \geq 0) \geq p_k \quad \text{for all } t \in [t_k, t_k + \tau_k), \quad (6)$$

where  $\mathbf{x}(t)$  follows the dynamics in (1), and  $p_k \in (0, 1)$  is a user-specified risk tolerance.

**Remark 1.** Problem 2 only addresses safety during the time interval  $[t_k, t_k + \tau_k)$ . As we will discuss in Remark 3, solving this problem also ensures safety with high probability along the system trajectory in a high-data regime, where sufficiently many samples are provided to the controller. In a low-data regime our design can be used in a hierarchical control design, as in [64], [65], alongside a high-level planner, such as Tube-MPC [13], [66], [67], RL-based control [16]–[18], [68], or a control contraction metric [69], [70], to guarantee safety. In this context, the high-level controller, which is computationally more expensive than our CBF-based controller, ensures safety along the system trajectory at a low frequency, and our CBF-based controller ensures safety short intervals, evaluated at higher frequency. •

## IV. MATRIX VARIATE GAUSSIAN PROCESS REGRESSION OF SYSTEM DYNAMICS

This section presents our solution to Problem 1. We aim to estimate the unknown drift  $f$  and input gain  $g$  of system (1)

<sup>1</sup>If not available, the derivatives may be approximated via finite differences, e.g.,  $\dot{\mathbf{X}}_{1:k} \triangleq \left[ \frac{\mathbf{x}(t_2) - \mathbf{x}(t_1)}{t_2 - t_1}, \dots, \frac{\mathbf{x}(t_{k+1}) - \mathbf{x}(t_k)}{t_{k+1} - t_k} \right]$ , provided that the inter-triggering times  $\{\tau_k = t_k - t_{k-1}\}_k$  are sufficiently small.



using a state-control dataset  $(\mathbf{X}_{1:k}, \mathbf{U}_{1:k}, \dot{\mathbf{X}}_{1:k})$ . To simplify the derivation, we assume that  $\mathbf{X}_{1:k}$  and  $\mathbf{U}_{1:k}$  are observed without noise but each measurement  $\dot{\mathbf{x}}(t_k)$  in  $\dot{\mathbf{X}}_{1:k}$  is corrupted by zero-mean Gaussian noise  $\mathcal{N}(\mathbf{0}, \mathbf{S})$  that is independent across time steps. Treating  $f(\mathbf{x}) + g(\mathbf{x})\mathbf{u}$  as a single vector-valued function with input  $[\mathbf{x}^\top, \mathbf{u}^\top]^\top$  may seem natural from a function approximation perspective but this approach ignores the control-affine structure. Encoding this structure in the learning process not only increases the learning efficiency but also ensures that the control Lyapunov and control barrier conditions remain linear in  $\mathbf{u}$ . Hence, we focus on learning the matrix-valued function  $F(\mathbf{x}) = [f(\mathbf{x}) \ g(\mathbf{x})]$  defined in (1).

The simplest approach is to use  $n(1+m)$  decoupled GPs for each element of  $F(\mathbf{x})$ . This approach ignores the dependencies among the components of  $f(\mathbf{x})$  and  $g(\mathbf{x})$ . Furthermore, since the outputs of  $f(\mathbf{x})$  and  $g(\mathbf{x})$  are observed together via  $\dot{\mathbf{X}}_{1:k}$ , training data dimensions are still mutually correlated and cannot be treated as decoupled GPs denying the efficiency advantage. At the other extreme, treating  $\text{vec}(F(\mathbf{x}))$  as a single vector-valued function and using a single GP distribution will enable high estimation accuracy but specifying an effective matrix-valued kernel function  $\mathbf{K}_0(\mathbf{x}, \mathbf{x}')$  and optimizing its hyperparameters is challenging. A promising approach is offered by the Coregionalization model [71], where the kernel function is decomposed as  $\mathbf{K}_0(\mathbf{x}, \mathbf{x}') \triangleq \Sigma \kappa_0(\mathbf{x}, \mathbf{x}')$  into a scalar kernel  $\kappa_0(\mathbf{x}, \mathbf{x}')$  and a covariance matrix parameter  $\Sigma \in \mathbb{R}^{n(1+m) \times (1+m)n}$ . Estimating  $\Sigma$  may still require a lot of training data. Moreover, the matrix-times-scalar-kernel structure is not preserved in the posterior of the Coregionalization model, preventing its effective use for incremental learning when new data is received over time.

We propose an alternative factorization of  $\mathbf{K}_0(\mathbf{x}, \mathbf{x}')$  inspired by the Matrix Variate Gaussian distribution [72], [73]. The strengths of our factorization are that it models the correlation among the elements of  $F(\mathbf{x})$ , preserves its structure in the posterior GP distribution, and has similar training and testing complexity as the decoupled GP approach.

**Definition 3.** The Matrix Variate Gaussian (MVG) distribution is a three-parameter distribution  $\mathcal{MN}(\mathbf{M}, \mathbf{A}, \mathbf{B})$  describing a random matrix  $\mathbf{X} \in \mathbb{R}^{n \times m}$  with probability density function:

$$p(\mathbf{X}; \mathbf{M}, \mathbf{A}, \mathbf{B}) \triangleq \frac{\exp\left(-\frac{1}{2} \text{tr}[\mathbf{B}^{-1}(\mathbf{X} - \mathbf{M})^\top \mathbf{A}^{-1}(\mathbf{X} - \mathbf{M})]\right)}{(2\pi)^{nm/2} \det(\mathbf{A})^{m/2} \det(\mathbf{B})^{n/2}}$$

where  $\mathbf{M} \in \mathbb{R}^{n \times m}$  is the mean and  $\mathbf{A} \in \mathbb{R}^{n \times n}$ ,  $\mathbf{B} \in \mathbb{R}^{m \times m}$  are the covariance matrices of the rows and columns of  $\mathbf{X}$ .

Additional properties of the MVG distribution are provided in Appendix A. Note that if  $\mathbf{X} \sim \mathcal{MN}(\mathbf{M}, \mathbf{A}, \mathbf{B})$ , then  $\text{vec}(\mathbf{X}) \sim \mathcal{N}(\text{vec}(\mathbf{M}), \mathbf{B} \otimes \mathbf{A})$ . Based on this observation, we propose the following decomposition of the GP prior:

$$\text{vec}(F(\mathbf{x})) \sim \mathcal{GP}(\text{vec}(\mathbf{M}_0(\mathbf{x})), \mathbf{B}_0(\mathbf{x}, \mathbf{x}') \otimes \mathbf{A}), \quad (7)$$

where  $\mathbf{B}_0(\mathbf{x}, \mathbf{x}') \in \mathbb{R}^{(m+1) \times (m+1)}$  and  $\mathbf{A} \in \mathbb{R}^{n \times n}$ . We assume that the noise covariance matrix satisfies  $\mathbf{S} = \sigma^2 \mathbf{A}$  for some parameter  $\sigma > 0$ . This assumption on the relationship between the measurement noise covariance  $\mathbf{S}$  and the dynam-

ics row covariance  $\mathbf{A}$  is necessary to preserve the Kronecker product structure of the covariance in the GP posterior.

To simplify notation, let  $\mathcal{B}_{1:k}^{1:k} \in \mathbb{R}^{k(m+1) \times k(m+1)}$  be a matrix with  $k \times k$  block elements  $[\mathcal{B}_{1:k}^{1:k}]_{i,j} \triangleq \mathbf{B}_0(\mathbf{x}_i, \mathbf{x}_j)$  and define  $\mathcal{M}_{1:k} \triangleq [\mathbf{M}_0(\mathbf{x}_1) \ \cdots \ \mathbf{M}_0(\mathbf{x}_k)] \in \mathbb{R}^{n \times k(m+1)}$ ,  $\mathcal{B}_{1:k}(\mathbf{x}) \triangleq [\mathbf{B}_0(\mathbf{x}, \mathbf{x}_1), \dots, \mathbf{B}_0(\mathbf{x}, \mathbf{x}_k)] \in \mathbb{R}^{(m+1) \times k(m+1)}$  and  $\mathcal{U}_{1:k} \triangleq \text{diag}(\mathbf{u}_1, \dots, \mathbf{u}_k) \in \mathbb{R}^{k(m+1) \times k}$ . Consider an arbitrary test point  $\mathbf{x}$ . The train and test data are jointly Gaussian:

$$\begin{bmatrix} \text{vec}(\dot{\mathbf{X}}_{1:k}) \\ \text{vec}(F(\mathbf{x})) \end{bmatrix} \sim \mathcal{N} \left( \begin{bmatrix} \text{vec}(\mathcal{M}_{1:k} \mathcal{U}_{1:k}) \\ \text{vec}(\mathbf{M}_0(\mathbf{x})) \end{bmatrix}, \begin{bmatrix} \mathcal{U}_{1:k}^\top \mathcal{B}_{1:k}^{1:k} \mathcal{U}_{1:k} + \sigma^2 \mathbf{I}_k & \mathcal{U}_{1:k}^\top \mathcal{B}_{1:k}(\mathbf{x}) \\ \mathcal{B}_{1:k}(\mathbf{x}) \mathcal{U}_{1:k} & \mathbf{B}_0(\mathbf{x}, \mathbf{x}) \end{bmatrix} \otimes \mathbf{A} \right), \quad (8)$$

where

$$\begin{aligned} \mathcal{U}_{1:k}^\top \mathcal{B}_{1:k}^{1:k} \mathcal{U}_{1:k} &= \begin{bmatrix} \mathbf{u}_1^\top \mathbf{B}_0(\mathbf{x}_1, \mathbf{x}_1) \mathbf{u}_1 & \cdots & \mathbf{u}_1^\top \mathbf{B}_0(\mathbf{x}_1, \mathbf{x}_k) \mathbf{u}_k \\ \vdots & \ddots & \vdots \\ \mathbf{u}_k^\top \mathbf{B}_0(\mathbf{x}_k, \mathbf{x}_1) \mathbf{u}_1 & \cdots & \mathbf{u}_k^\top \mathbf{B}_0(\mathbf{x}_k, \mathbf{x}_k) \mathbf{u}_k \end{bmatrix} \\ \mathcal{B}_{1:k}(\mathbf{x}) \mathcal{U}_{1:k} &= [\mathbf{B}_0(\mathbf{x}_1, \mathbf{x}) \mathbf{u}_1 \ \cdots \ \mathbf{B}_0(\mathbf{x}_k, \mathbf{x}) \mathbf{u}_k]. \end{aligned} \quad (9)$$

Applying a Schur complement to (8), we find the distribution of  $\text{vec}(F(\mathbf{x}))$  conditioned on  $(\mathbf{X}_{1:k}, \mathbf{U}_{1:k}, \dot{\mathbf{X}}_{1:k})$ .

**Proposition 3.** The posterior distribution of  $\text{vec}(F(\mathbf{x}))$  conditioned on the training data  $(\mathbf{X}_{1:k}, \mathbf{U}_{1:k}, \dot{\mathbf{X}}_{1:k})$  is a Gaussian process  $\mathcal{GP}(\text{vec}(\mathbf{M}_k(\mathbf{x})), \mathbf{B}_k(\mathbf{x}, \mathbf{x}') \otimes \mathbf{A})$  with parameters:

$$\begin{aligned} \mathbf{M}_k(\mathbf{x}) &\triangleq \mathbf{M}_0(\mathbf{x}) + \left( \dot{\mathbf{X}}_{1:k} - \mathcal{M}_{1:k} \mathcal{U}_{1:k} \right) (\mathcal{U}_{1:k}^\top \mathcal{B}_{1:k}(\mathbf{x}))^\dagger \\ \mathbf{B}_k(\mathbf{x}, \mathbf{x}') &\triangleq \mathbf{B}_0(\mathbf{x}, \mathbf{x}') - \mathcal{B}_{1:k}(\mathbf{x}) \mathcal{U}_{1:k} (\mathcal{U}_{1:k}^\top \mathcal{B}_{1:k}(\mathbf{x}'))^\dagger \\ (\mathcal{U}_{1:k}^\top \mathcal{B}_{1:k}(\mathbf{x}))^\dagger &\triangleq \left( \mathcal{U}_{1:k}^\top \mathcal{B}_{1:k}^{1:k} \mathcal{U}_{1:k} + \sigma^2 \mathbf{I}_k \right)^{-1} \mathcal{U}_{1:k}^\top \mathcal{B}_{1:k}^\top(\mathbf{x}). \end{aligned} \quad (10)$$

*Proof.* See Appendix B.  $\square$

Thm. 3 shows that, for a given control input  $\mathbf{u}$ , the MVGP posterior of  $F(\mathbf{x})\mathbf{u}$  is (applying Lemma 5):

$$F(\mathbf{x})\mathbf{u} \sim \mathcal{GP}(\mathbf{M}_k(\mathbf{x})\mathbf{u}, \mathbf{u}^\top \mathbf{B}_k(\mathbf{x}, \mathbf{x}') \mathbf{u} \otimes \mathbf{A}). \quad (11)$$

A key property of the MVGP model in Thm. 3 is that the posterior preserves the kernel decomposition. Letting  $\mathbf{B}_0(\mathbf{x}, \mathbf{x}') \triangleq \mathbf{B}_0 \kappa_0(\mathbf{x}, \mathbf{x}')$ , in addition to the kernel parameters, our model requires learning of  $\mathbf{B} \in \mathbb{R}^{(1+m) \times (1+m)}$  and, if the measurement noise statistics are unknown,  $\mathbf{A} \in \mathbb{R}^{n \times n}$  and  $\sigma \in \mathbb{R}$ . Thus, the MVGP model has fewer parameters than a Coregionalization model, which requires  $(1+m)^2 n^2$  parameters for the full covariance decomposition  $\mathbf{K}_0(\mathbf{x}, \mathbf{x}') \triangleq \Sigma \kappa_0(\mathbf{x}, \mathbf{x}')$ . For a data set with  $k$  examples, the training computational complexity of our MVGP approach is  $O(k^3)$ , while the same for the Coregionalization model is  $O(k^3 n^3)$ . This is because our model inverts only a  $(k \times k)$  matrix while the Coregionalization model inverts a  $(kn \times kn)$  matrix (see Appendix C). The accuracy and computational complexity of the MVGP model and the Coregionalization model are compared in Sec. VIII-A.

## V. SELF-TRIGGERED CONTROL WITH PROBABILISTIC SAFETY CONSTRAINTS

The MVGP model developed in Sec. IV addresses Problem 1 and provides a probabilistic estimate of the unknown system dynamics  $F(\mathbf{x})\underline{\mathbf{u}}$  in (11). In this section, we consider Problem 2. We extend the optimization-based control synthesis approach in (4) to handle probabilistic stability and safety constraints induced by the posterior distribution of  $F(\mathbf{x})\underline{\mathbf{u}}$ . We focus on handling probabilistic safety constraints of the form  $\mathbb{P}(\text{CBC}(\mathbf{x}, \underline{\mathbf{u}}) \geq 0) \geq p$ . Since the control Lyapunov and control barrier conditions have the same form, involving the Lie derivative of a known function  $V(\mathbf{x})$  or  $h(\mathbf{x})$  with respect to the system dynamics, our approach can be used for stability constraints as well, as demonstrated in Sec. VIII-B. Furthermore, we develop self-triggering conditions to adaptively decide the times  $t_k, t_{k+1}, \dots$ , at which the system inputs  $\underline{\mathbf{u}}$  should be recomputed in order to guarantee safety with high probability along the continuous-time system trajectory, instead of instantaneously in time.

Our approach requires that the sample paths of the GP used to model the unknown system dynamics  $F(\mathbf{x})\underline{\mathbf{u}}$  are locally Lipschitz with high probability.

**Assumption 1.** Let  $\mathbb{P}_k$  be the probability measure induced by the distribution of  $F(\mathbf{x})\underline{\mathbf{u}}$  at time  $t_k$ . Assume that for any  $L_k > 0$ ,  $\underline{\mathbf{u}}$ , and  $\tau_k$ , there exists a constant  $b_k > 0$  such that:

$$\mathbb{P}_k \left( \sup_{s \in [0, \tau_k]} \|F(\mathbf{x}(t_k + s))\underline{\mathbf{u}}_k - F(\mathbf{x}(t_k))\underline{\mathbf{u}}_k\| \leq L_k \|\mathbf{x}(t_k + s) - \mathbf{x}(t_k)\| \right) \geq q_k \triangleq 1 - e^{-b_k L_k}. \quad (12)$$

Assumption 1 holds for a large class of GPs, such as those with stationary kernels that are four times differentiable, including squared exponential and some Matérn kernels [74], [75]. However, it may not hold for GPs with highly erratic sample paths. Similar smoothness assumptions have been used in [76], [77].

### A. Probabilistic Safety Constraints

Consider probabilistic stability and safety constraints in the CLF-CBF QP in (4), induced by the MVGP distribution of  $F(\mathbf{x})\underline{\mathbf{u}}$  at time  $t_k$  in (11):

$$\begin{aligned} \pi(\mathbf{x}_k) \in \arg \min_{\underline{\mathbf{u}}_k \in \mathcal{U}, \delta \in \mathbb{R}} \|\mathbf{R}(\mathbf{x}_k)\underline{\mathbf{u}}_k\|^2 + \lambda \delta^2 \\ \text{s.t. } \mathbb{P}(\text{CLC}(\mathbf{x}_k, \underline{\mathbf{u}}_k) \leq \delta \mid \mathbf{x}_k, \underline{\mathbf{u}}_k) \geq \tilde{p}_k \\ \mathbb{P}(\text{CBC}(\mathbf{x}_k, \underline{\mathbf{u}}_k) \geq \zeta \mid \mathbf{x}_k, \underline{\mathbf{u}}_k) \geq \tilde{p}_k, \end{aligned} \quad (13)$$

where  $\tilde{p}_k = p_k/q_k$ . To ensure that the safety constraint does not only hold instantaneously in time but over a time interval  $[t_k, t_k + \tau_k]$ , we enforce a tighter constraint via  $\zeta > 0$  and determine the time  $\tau_k$  for which it remains valid. The choice of  $\zeta$  and its effect on  $\tau_k$  are discussed next.

**Lemma 1.** Consider the dynamics in (1) with posterior distribution in (11). Given  $\mathbf{x}_k$  and  $\underline{\mathbf{u}}_k$ ,  $\text{CBC}_k \triangleq \text{CBC}(\mathbf{x}_k, \underline{\mathbf{u}}_k)$  is a Gaussian random variable with the following parameters:

$$\mathbb{E}[\text{CBC}_k] = \nabla_{\mathbf{x}} h(\mathbf{x}_k)^\top \mathbf{M}_k(\mathbf{x}_k)\underline{\mathbf{u}}_k + \alpha(h(\mathbf{x}_k)), \quad (14)$$

$$\text{Var}[\text{CBC}_k] = (\underline{\mathbf{u}}_k^\top \mathbf{B}_k(\mathbf{x}_k, \mathbf{x}_k)\underline{\mathbf{u}}_k)(\nabla_{\mathbf{x}} h(\mathbf{x}_k)^\top \mathbf{A} \nabla_{\mathbf{x}} h(\mathbf{x}_k))$$

*Proof.* We start by re-writing the definition of CBC as follows.

$$\text{CBC}_k = \nabla_{\mathbf{x}} h(\mathbf{x}_k)^\top F_k(\mathbf{x}_k)\underline{\mathbf{u}}_k + \alpha(h(\mathbf{x}_k)). \quad (15)$$

The mean and variance of  $\text{CBC}_k$  can be written as,

$$\begin{aligned} \mathbb{E}[\text{CBC}_k] &= \nabla_{\mathbf{x}} h(\mathbf{x}_k)^\top \mathbb{E}[F_k(\mathbf{x}_k)\underline{\mathbf{u}}_k] + \alpha(h(\mathbf{x}_k)), \\ \text{Var}[\text{CBC}_k] &= \nabla_{\mathbf{x}} h(\mathbf{x}_k)^\top \text{Var}(F_k(\mathbf{x}_k)\underline{\mathbf{u}}_k) \nabla_{\mathbf{x}} h(\mathbf{x}_k), \end{aligned} \quad (16)$$

where the mean and variance of  $F(\mathbf{x}_k)\underline{\mathbf{u}}_k$  are available from (11).  $\square$

Using Lemma 1, we can rewrite the safety constraint as

$$\mathbb{P}(\text{CBC}_k \geq \zeta \mid \mathbf{x}_k, \underline{\mathbf{u}}_k) = 1 - \Phi \left( \frac{\zeta - \mathbb{E}[\text{CBC}_k]}{\sqrt{\text{Var}[\text{CBC}_k]}} \right) \geq \tilde{p}_k, \quad (17)$$

where  $\Phi(\cdot)$  is the cumulative distribution function of the standard Gaussian. Note that if the control input is chosen so that  $\frac{\zeta - \mathbb{E}[\text{CBC}_k]}{\sqrt{\text{Var}[\text{CBC}_k]}} \rightarrow -\infty$ , as the posterior variance of  $\text{CBC}_k$  tends to zero, the probability  $\mathbb{P}(\text{CBC}_k \geq \zeta \mid \mathbf{x}_k, \underline{\mathbf{u}}_k)$  tends to one. Namely, as the uncertainty about the system dynamics tends to zero, our results reduce to the setting of Sec. III-B, and safety can be ensured with probability one. Using (17) and noting that  $\Phi^{-1}(1 - \tilde{p}_k) = -\sqrt{2}\text{erf}^{-1}(2\tilde{p}_k - 1)$ , the optimization problem in (13) can be restated as

$$\begin{aligned} \pi(\mathbf{x}_k) \in \arg \min_{\underline{\mathbf{u}}_k \in \mathcal{U}, \delta \in \mathbb{R}} \|\mathbf{R}(\mathbf{x}_k)\underline{\mathbf{u}}_k\|^2 + \lambda \delta^2 \\ \text{s.t. } \delta - \mathbb{E}[\text{CLC}_k] \geq c(\tilde{p}_k) \sqrt{\text{Var}[\text{CLC}_k]} \\ \zeta - \mathbb{E}[\text{CBC}_k] \leq -c(\tilde{p}_k) \sqrt{\text{Var}[\text{CBC}_k]}, \end{aligned} \quad (18)$$

where  $c(\tilde{p}_k) \triangleq \sqrt{2}\text{erf}^{-1}(2\tilde{p}_k - 1)$ .

**Proposition 4.** The chance-constrained optimization problem in (13) for control-affine system dynamics in (1) with posterior distribution (11) is a second-order cone program (SOCP):

$$\pi(\mathbf{x}_k) \in \arg \min_{y \in \mathbb{R}, \delta \in \mathbb{R}, \underline{\mathbf{u}} \in \mathcal{U}} y \quad (19a)$$

$$\text{s.t. } y - \left\| \mathbf{R}(\mathbf{x}_k)\underline{\mathbf{u}} + \sqrt{\lambda}\delta \right\|_2 \geq 0 \quad (19b)$$

$$\mathbf{q}_k(\mathbf{x}_k)^\top \underline{\mathbf{u}} - \delta + c(\tilde{p}_k) \|\mathbf{P}_k(\mathbf{x}_k)\underline{\mathbf{u}}\|_2 \leq 0 \quad (19c)$$

$$\mathbf{e}_k(\mathbf{x}_k)^\top \underline{\mathbf{u}} - \zeta - c(\tilde{p}_k) \|\mathbf{V}_k(\mathbf{x}_k)\underline{\mathbf{u}}\|_2 \geq 0, \quad (19d)$$

where

$$\mathbf{q}_k(\mathbf{x}_k) \triangleq \mathbf{M}_k(\mathbf{x}_k)^\top \nabla_{\mathbf{x}} V(\mathbf{x}_k) + \begin{bmatrix} \gamma(V(\mathbf{x}_k)) \\ \mathbf{0}_m \end{bmatrix},$$

$$\mathbf{P}_k(\mathbf{x}_k) \triangleq \sqrt{\nabla_{\mathbf{x}} V(\mathbf{x}_k)^\top \mathbf{A} \nabla_{\mathbf{x}} V(\mathbf{x}_k) \mathbf{B}_k^{\frac{1}{2}}(\mathbf{x}_k, \mathbf{x}_k)},$$

$$\mathbf{e}_k(\mathbf{x}_k) \triangleq \mathbf{M}_k(\mathbf{x}_k)^\top \nabla_{\mathbf{x}} h(\mathbf{x}_k) + \begin{bmatrix} \alpha(h(\mathbf{x}_k)) \\ \mathbf{0}_m \end{bmatrix},$$

$$\mathbf{V}_k(\mathbf{x}_k) \triangleq \sqrt{\nabla_{\mathbf{x}} h(\mathbf{x}_k)^\top \mathbf{A} \nabla_{\mathbf{x}} h(\mathbf{x}_k) \mathbf{B}_k^{\frac{1}{2}}(\mathbf{x}_k, \mathbf{x}_k)},$$

and  $\mathbf{B}_k^{\frac{1}{2}}(\mathbf{x}_k, \mathbf{x}_k)$  is the Cholesky factorization of  $\mathbf{B}_k(\mathbf{x}_k, \mathbf{x}_k)$ .

*Proof.* Substituting the mean and variance of  $\text{CLC}_k$  and  $\text{CBC}_k$  (c.f. Lemma 1) into (18) and introducing an auxiliary variable  $y$  to express the quadratic objective as a SOCP constraint leads to the result.  $\square$

We refer to the left-hand side of the constraints in (19d) and (19c) as Stochastic CBC (SCBC) and Stochastic CLC (SCLC), respectively. Note that when  $\tilde{p}_k = 0.5$ ,  $c(\tilde{p}_k) = 0$  and the SOCP in (19) reduces to the deterministic-case QP in (4). Otherwise, the SOCP can be solved to arbitrary precision  $\epsilon$  within  $O(-\log(\epsilon))$  iterations [78] with off-the-shelf solvers, e.g., GUROBI [79], CVXOPT [80].

*Remark 2.* In the conference version of this work [1], the probabilistic safety constraint in (13) was formulated in a Quadratically Constrained Quadratic Program (QCQP):

$$\begin{aligned} \min_{\mathbf{u}_k} & \mathbf{u}_k^\top \mathbf{R}(\mathbf{x}_k)^\top \mathbf{R}(\mathbf{x}_k) \mathbf{u}_k \\ \text{s.t.} & \mathbf{u}_k^\top (c(\tilde{p}_k) \mathbf{V}(\mathbf{x}_k)^\top \mathbf{V}(\mathbf{x}_k) - \mathbf{e}(\mathbf{x}_k) \mathbf{e}(\mathbf{x}_k)^\top) \mathbf{u}_k \\ & - 2(\alpha(h(\mathbf{x}_k)) - \zeta) \mathbf{e}(\mathbf{x}_k)^\top \mathbf{u} - (\alpha(h(\mathbf{x}_k)) - \zeta)^2 \leq 0. \end{aligned}$$

However, for this QCQP to be convex, the matrix  $c(\tilde{p}_k) \mathbf{V}(\mathbf{x}_k)^\top \mathbf{V}(\mathbf{x}_k) - \mathbf{e}(\mathbf{x}_k) \mathbf{e}(\mathbf{x}_k)^\top$  must be positive definite. This is true only when the smallest eigenvalue of the CBC variance  $c(\tilde{p}_k) \mathbf{V}(\mathbf{x}_k)^\top \mathbf{V}(\mathbf{x}_k)$  is greater than the magnitude of the CBC expectation  $\|\mathbf{e}(\mathbf{x}_k)\|_2^2$ . This is not guaranteed, especially when the CBC variance is small. While there exist solvers for non-convex QCQPs [79], there are no global convergence guarantees for non-convex problems and, hence, safety cannot be guaranteed. •

### B. Self-triggering Design

The safety constraint in (19) ensures safety with high probability at the triggering times  $\{t_k\}_{k \in \mathbb{N}}$ . Here, we extend our analysis to the inter-triggering intervals  $[t_k, t_k + \tau_k)$ . We continue by re-stating [30, Proposition 1] in our setting.

**Proposition 5.** *Consider the system in (1) with zero-order hold control in inter-triggering times. If the event in (12) occurs at the  $k$ -th triggering time, then for all  $s \in [0, \tau_k)$  we have:*

$$\|\mathbf{x}(t_k + s) - \mathbf{x}_k\| \leq \bar{r}_k(s) \triangleq \frac{1}{L_k} \|\dot{\mathbf{x}}_k\| (e^{L_k s} - 1). \quad (20)$$

Recall from Sec. III-B that  $h$  is a continuously differentiable function. Thus, using Proposition 5, we notice, for any inter-triggering time  $\tau_k$ , there exist a constant  $\chi_k > 0$  such that

$$\sup_{s \in [0, \tau_k)} \|\nabla_{\mathbf{x}} h(\mathbf{x}(t_k + s))\| \leq \chi_k. \quad (21)$$

This is used in the next theorem which concerns Problem 2.

**Proposition 6.** *Consider the system in (1) with safe set  $\mathcal{C}$ . Assume the SOCP in (19) has a solution at triggering time  $t_k$ , the event in (12) occurs at least with probability  $q_k$ , and for all  $s \in [0, \tau_k)$ ,  $\alpha \circ h$  satisfies the following Lipschitz property*

$$|\alpha(h(\mathbf{x}(t_k + s))) - \alpha(h(\mathbf{x}_k))| \leq L_{\alpha \circ h} \|\mathbf{x}(t_k + s) - \mathbf{x}_k\|. \quad (22)$$

*Then, the constraint in (6) is satisfied with  $p_k = \tilde{p}_k q_k$  for  $\tau_k \leq \frac{1}{L_k} \ln \left( 1 + \frac{L_k \zeta}{(\chi_k L_k + L_{\alpha \circ h}) \|\dot{\mathbf{x}}_k\|} \right)$ , where  $\chi_k$  is given in (21).*

*Proof.* Since the program (13) has a solution at the triggering time  $t_k$  we know  $\mathbb{P}(\text{CBC}_k \geq \zeta | \mathbf{x}_k, \mathbf{u}_k) \geq \tilde{p}_k$ . Thus, conditioned on  $\text{CBC}_k \geq \zeta$ , and the event (12), if we prove  $\text{CBC}(s + t_k) \geq 0$ , for all  $s \in [0, \tau_k)$ , the result follows. Using the Cauchy-Schwarz inequality, the Lipschitz continuity

assumptions in (12) and (22), and Proposition 5, for all  $s \in [0, \tau_k)$ , we have:

$$|\text{CBC}(\mathbf{x}(s + t_k), \mathbf{u}_k) - \text{CBC}_k| \leq \left( \sup_{s \in [0, \tau_k)} \|\nabla_{\mathbf{x}} h(\mathbf{x}(s + t_k))\| L_k + L_{\alpha \circ h} \right) \bar{r}_k(s). \quad (23)$$

Thus, using (20) and (21), we notice that the right-hand side of (23) is upper-bounded by

$$\frac{\chi_k L_k + L_{\alpha \circ h}}{L_k} \|\dot{\mathbf{x}}_k\| (e^{L_k s} - 1), \quad (24)$$

which, in turn, is less than or equal to  $\zeta$  for  $s = \tau_k$ . □

Assuming that the Lipschitz property in (12) occurs with probability at least  $q_k$  and given the value of  $\|\dot{\mathbf{x}}_k\|$  at triggering time  $t_k$  and the parameters  $\zeta$  in (13),  $\chi_k$  in (21), and  $L_{\alpha \circ h}$  in (22), Proposition 6 characterizes the longest time until it is necessary to recompute the control input to guarantee safety with probability at least  $p_k = \tilde{p}_k q_k$ .

*Remark 3.* Under appropriate assumptions [75], [81], the posterior variance of a GP with Lipschitz continuous kernel converges to zero at any query point, given a sufficiently large set of training data around that query point. In this high-data regime,  $\text{Var}[\text{CBC}_k]$  in (14) tends to zero and the user-specified safety tolerance  $\tilde{p}_k$  in (17) can be set arbitrary close to one. In this context, our approach can ensure safety with arbitrarily high probability along the system trajectory for arbitrarily time intervals, provided that the true model is Lipschitz continuous according to (12). Finding a non-trivial lower bound on the safety probability with limited training data across multiple inter-triggering intervals along the system trajectory is an interesting research problem [82]–[86] that we leave for future work. •

## VI. EXTENSION TO HIGHER RELATIVE-DEGREE SYSTEMS

Next, we extend the probabilistic safety constraint formulation for systems with arbitrary relative degree<sup>2</sup>, using an exponential control barrier function (ECBF) [25], [37]. Sec. VI-A reviews ECBF results for systems with *known dynamics*. Sec. VI-B investigate probabilistic ECBF constraints, while Sec. VI-C provides a self-triggering formulation.

### A. Known Dynamics

Let  $r \geq 1$  be the relative degree of (1) with respect to  $h(\mathbf{x})$ , i.e.,  $\mathcal{L}_g \mathcal{L}_f^{(r-1)} h(\mathbf{x}) \neq 0$  and  $\mathcal{L}_g \mathcal{L}_f^{(k-1)} h(\mathbf{x}) = 0$ ,  $\forall k \in \{1, \dots, r-2\}$ . This condition can be expressed by defining

$$\boldsymbol{\eta}(\mathbf{x}) \triangleq \begin{bmatrix} h(\mathbf{x}) \\ \mathcal{L}_f h(\mathbf{x}) \\ \vdots \\ \mathcal{L}_f^{(r-1)} h(\mathbf{x}) \end{bmatrix}, \quad \mathcal{F} \triangleq \begin{bmatrix} 0 & 1 & \dots & 0 \\ \vdots & \vdots & & \vdots \\ 0 & 0 & \dots & 1 \\ 0 & 0 & \dots & 0 \end{bmatrix}, \quad \mathcal{G} \triangleq \begin{bmatrix} 0 \\ \vdots \\ 0 \\ 1 \end{bmatrix}$$

<sup>2</sup>The motivation for assuming known relative degree but unknown dynamics comes from robotics applications. Commonly, the class of the system is known but the parameters (e.g., mass, moment of inertia) and high-order interactions (e.g., jerk, snap, drag) of the dynamics are unknown. Estimating the relative degree is left for future work (cf. [87]–[89]).

and specifying  $h(\mathbf{x})$  as the output of the linear time-invariant system:

$$\dot{\boldsymbol{\eta}}(\mathbf{x}) = \mathcal{F}\boldsymbol{\eta}(\mathbf{x}) + \mathcal{G}\mathbf{u}, \quad h(\mathbf{x}) = \mathbf{c}^\top \boldsymbol{\eta}(\mathbf{x}), \quad (25)$$

where  $\mathbf{c} \triangleq [1, 0, \dots, 0]^\top \in \mathbb{R}^r$ .

**Definition 4** ([25], [37]). A function  $h \in \mathbb{C}^r(\mathcal{X}, \mathbb{R})$  is an exponential control barrier function (ECBF) for the system in (1) if there exists a vector  $\mathbf{k}_\alpha \in \mathbb{R}^r$  such that the  $r$ -th order control barrier condition  $\text{CBC}^{(r)}(\mathbf{x}, \mathbf{u}) \triangleq \mathcal{L}_f^{(r)}h(\mathbf{x}) + \mathcal{L}_g\mathcal{L}_f^{(r-1)}h(\mathbf{x})\mathbf{u} + \mathbf{k}_\alpha^\top \boldsymbol{\eta}(\mathbf{x})$  satisfies  $\sup_{\mathbf{u} \in \mathcal{U}} \text{CBC}^{(r)}(\mathbf{x}, \mathbf{u}) \geq 0$  for all  $\mathbf{x} \in \mathcal{X}$  and  $h(\mathbf{x}(t)) \geq \mathbf{c}^\top \boldsymbol{\eta}(\mathbf{x}_0)e^{(\mathcal{F}-\mathcal{G}\mathbf{k}_\alpha)t} \geq 0$ , whenever  $h(\mathbf{x}(0)) \geq 0$ .

If  $\mathbf{k}_\alpha$  satisfies the properties from [37, Thm. 2], then any control policy  $\mathbf{u} = \pi(\mathbf{x})$  that ensures  $\text{CBC}^{(r)}(\mathbf{x}, \mathbf{u}) \geq 0$  renders the dynamics (1) safe with respect to  $\mathcal{C} = \{\mathbf{x} \in \mathcal{X} \mid h(\mathbf{x}) \geq 0\}$ . For relative-degree-one systems,  $\mathbf{k}_\alpha^\top \boldsymbol{\eta}(\mathbf{x})$  reduces to  $\alpha h(\mathbf{x})$  with  $\alpha > 0$ . Thus,  $\text{CBC}^{(1)}$ , the safety condition based on ECBF for  $r = 1$ , is equivalent to the CBC in Def. 2 when the extended class  $K_\infty$  function  $\alpha$  is linear.

### B. Probabilistic ECBF Constraints

As in (13), we are interested in solving

$$\begin{aligned} \pi(\mathbf{x}_k) \in \arg \min_{\mathbf{u}_k \in \mathcal{U}} \|\mathbf{R}(\mathbf{x}_k)\mathbf{u}_k\|_2 \\ \text{s.t. } \mathbb{P}(\text{CBC}_k^{(r)} \geq \zeta | \mathbf{x}_k, \mathbf{u}_k) \geq \tilde{p}_k, \end{aligned} \quad (26)$$

where  $\text{CBC}_k^{(r)} \triangleq \text{CBC}^{(r)}(\mathbf{x}_k, \mathbf{u}_k)$  and we have dropped the CLC term for clarity of presentation. While we explicitly characterised the distribution of  $\text{CBC}_k$  for relative degree one in Lemma 1, the distribution of  $\text{CBC}_k^{(r)}$  cannot be determined explicitly for arbitrary  $r$ . Instead, we use a concentration bound to rewrite the chance constraint in terms of the moments of  $\text{CBC}_k^{(r)}$ .

**Proposition 7.** Let  $r \geq 1$  be the relative degree of (1) with respect to  $h(\mathbf{x}) \in \mathbb{C}^r(\mathcal{X}, \mathbb{R})$  and  $F(\mathbf{x})$  be a random function with finite mean and variance. Then, the expectation and variance of  $\text{CBC}^{(r)}(\mathbf{x}, \mathbf{u})$  in Def. 4 are linear and quadratic in  $\mathbf{u}$ , respectively, and satisfy:

$$\begin{aligned} \mathbb{E}[\text{CBC}^{(r)}(\mathbf{x}, \mathbf{u})] &= \mathbf{e}^{(r)}(\mathbf{x})^\top \mathbf{u}, \\ \text{Var}[\text{CBC}^{(r)}(\mathbf{x}, \mathbf{u})] &= \mathbf{u}^\top \mathbf{V}^{(r)}(\mathbf{x}) \mathbf{V}^{(r)}(\mathbf{x})^\top \mathbf{u}, \end{aligned} \quad (27)$$

where

$$\mathbf{e}^{(r)}(\mathbf{x}) \triangleq \mathbb{E} \left[ F(\mathbf{x})^\top \nabla_{\mathbf{x}} \mathcal{L}_f^{(r-1)} h(\mathbf{x}) + \begin{bmatrix} \mathbf{k}_\alpha^\top \boldsymbol{\eta}(\mathbf{x}) \\ \mathbf{0}_m \end{bmatrix} \right] \quad (28)$$

$$\mathbf{V}^{(r)}(\mathbf{x}) \triangleq \text{Var} \left[ F(\mathbf{x})^\top \nabla_{\mathbf{x}} \mathcal{L}_f^{(r-1)} h(\mathbf{x}) + \begin{bmatrix} \mathbf{k}_\alpha^\top \boldsymbol{\eta}(\mathbf{x}) \\ \mathbf{0}_m \end{bmatrix} \right]^\frac{1}{2} \quad (29)$$

*Proof.* See Appendix D.  $\square$

**Proposition 8.** Consider the control-affine system in (1) with relative degree  $r \geq 1$  with respect to an ECBF  $h(\mathbf{x}) \in \mathbb{C}^r(\mathcal{X}, \mathbb{R})$ . If the system inputs are determined in continuous time  $t_k$  from the following SOCP,

$$\pi(\mathbf{x}_k) \in \arg \min_{y \in \mathbb{R}, \mathbf{u}_k \in \mathcal{U}} y$$

$$\text{s.t. } y - \|\mathbf{R}(\mathbf{x}_k)\mathbf{u}_k\|_2 \geq 0 \quad (30)$$

$$\mathbf{e}_k^{(r)}(\mathbf{x}_k)^\top \mathbf{u}_k - \zeta - c^{(r)}(\tilde{p}_k) \left\| \mathbf{V}_k^{(r)}(\mathbf{x}_k) \mathbf{u}_k \right\|_2 \geq 0,$$

where  $c^{(r)}(\tilde{p}_k) \triangleq \sqrt{\frac{\tilde{p}_k}{1-\tilde{p}_k}}$  and  $\tilde{p}_k \in (0, 1)$  is fixed for all  $t_k$ , then the system trajectory remains in the safe set  $\mathcal{C} = \{\mathbf{x} \in \mathcal{X} \mid h(\mathbf{x}) \geq 0\}$  with probability  $\tilde{p}_k$ .

*Proof.* See Appendix E.  $\square$

In the proposition above, we bound  $\mathbb{P}(\text{CBC}_k^{(r)} \geq \zeta | \mathbf{x}_k, \mathbf{u}_k)$  in (26) using Cantelli's inequality, because the exact distribution of  $\text{CBC}_k^{(r)}$  is unknown. The safety constraint in (30) can be interpreted as: "The system must satisfy  $\text{CBC}_k^{(r)}$  in expectation by a margin  $c(\tilde{p}_k)$  times the standard deviation of  $\text{CBC}_k^{(r)}$ ". Solving the SOCP requires knowledge of the mean and variance of  $\text{CBC}_k^{(r)}$ . Sec. VII shows how to determine the mean and variance of  $\text{CBC}_k^{(2)}$ , which is of practical relevance for many physical systems. For  $r > 2$ , Monte Carlo sampling can be used to estimate these quantities.

### C. Self-triggering Design

In this section, we extend the time-triggered formulation for probabilistic safety of high relative degree systems to a self-triggering setup. Our extension to self-triggering control in the relative-degree-one case in Proposition 6, relied on Lipschitz continuity of the CBC components. To simplify the analysis for arbitrary relative degree  $r$ , we temporarily introduce a modified CBF  $h_b(\mathbf{x}) \triangleq h(\mathbf{x}) - \zeta_b$  with  $\zeta_b > 0$ . We solve the SOCP in (30) with  $\zeta = 0$  but replace  $h(\mathbf{x})$  with  $h_b(\mathbf{x})$ . Enforcing the safety constraint in (30) for  $h_b(\mathbf{x}_k)$ , ensures that with probability  $\tilde{p}_k$ ,  $h(\mathbf{x}_k) \geq \zeta_b$  at the sampling times. We find an upper bound on the sampling time  $\tau_k$  that ensures  $h(\mathbf{x}(t))$  remains non-negative during the inter-triggering intervals  $[t_k, t_k + \tau_k)$ .

**Proposition 9.** Consider the system in (1) with safe set  $\mathcal{C} = \{\mathbf{x} \in \mathcal{X} \mid h(\mathbf{x}) \geq 0\}$ . Assume the SOCP in (30) has a solution at triggering time  $t_k$  with  $h_b(\mathbf{x}) \triangleq h(\mathbf{x}) - \zeta_b$  as the CBF and  $\zeta = 0$ . Suppose that event (12) occurs at least with probability  $q_k$  and for all  $s \in [0, \tau_k)$ ,  $h$  satisfies the following Lipschitz property

$$\sup_{s \in [0, \tau_k)} |h(\mathbf{x}(t_k + s)) - h(\mathbf{x}_k)| \leq L_h \|\mathbf{x}(t_k + s) - \mathbf{x}_k\|. \quad (31)$$

Then, the constraint in (6) is valid for  $p_k = \tilde{p}_k q_k$ , and  $\tau_k \leq \frac{1}{L_k} \ln \left( 1 + \frac{L_k \zeta_b}{L_h \|\dot{\mathbf{x}}_k\|} \right)$ .

*Proof.* Using Proposition 5 and (31) we have

$$\begin{aligned} \sup_{s \in [0, \tau_k)} |h(\mathbf{x}(t_k + s)) - h(\mathbf{x}_k)| &\leq L_h \|\mathbf{x}(t_k + s) - \mathbf{x}_k\| \\ &\leq \frac{L_h}{L_k} \|\dot{\mathbf{x}}_k\| (e^{L_k \tau_k} - 1) \leq \zeta_b, \end{aligned} \quad (32)$$

where the last inequality follows from the upper bound on  $\tau_k$ . Given  $h(\mathbf{x}(t)) \geq \zeta_b$  at the triggering time  $t_k$ , we deduce  $h(\mathbf{x}(t)) \geq 0$  for all time in  $[t_k, t_{k+1})$ , and the result follows.  $\square$



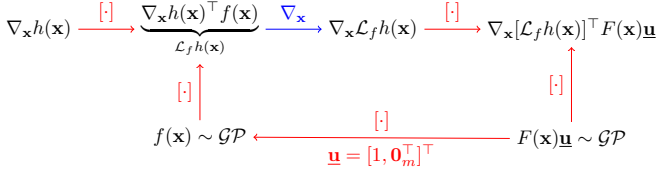


Fig. 2. Computation graph for the second-order Lie derivative of a control barrier function  $h(x)$  along the GP-distributed dynamics  $F(x)\underline{u}$  of a relative degree two system. Only two kinds of operations are required: (1) dot product with a vector-variate GP ([:]) and (2) gradient of a scalar GP ( $\nabla_x$ ).

Assuming that the Lipschitz property in (12) occurs with probability at least  $q_k$ , and given the value of  $\|\dot{x}_k\|$  at triggering time  $t_k$  and the parameter  $\zeta_b > 0$  and the Lipschitz constant  $L_h$  in (22), Proposition 9 characterizes the longest time  $\tau_k$  until a control input needs to be recomputed to guarantee safety with probability at least  $p_k = \bar{p}_k q_k$  for a system with arbitrary relative degree.

*Remark 4.* Recent works [90]–[92] study a more general high-order CBF (HOCBF) formulation than ECBF. Applying our probabilistic safety constraints with a HOCBF is left for future work.

## VII. SPECIAL CASE: RELATIVE DEGREE TWO

Systems with relative degree two appear frequently. We develop an efficient approach for computing the mean and variance of  $\text{CBC}^{(r)}$  for  $r \leq 2$ , which is needed to specify the safety constraints in our SOCP formulation in (30). The mean and variance of  $\text{CBC}^{(1)}$  are provided in Lemma 1. Here, we compute the mean and variance of  $\text{CBC}^{(2)}$ :

$$\text{CBC}^{(2)}(x, u) = [\nabla_x \mathcal{L}_f h(x)]^\top F(x)\underline{u} + [h(x), \mathcal{L}_f h(x)]^\top \mathbf{k}_\alpha. \quad (33)$$

Note that  $\text{CBC}^{(2)}(x, u)$  is a stochastic process whose distribution is induced by the Gaussian Process  $\text{vec}(F(x))$ . In Fig 2, we represent (33) as a computation graph with random or deterministic functions as nodes and computations among them as edges. The graph contains only two kinds of edges: (1) dot product of a deterministic function with a vector-variate GP and (2) gradient of a scalar GP. We show how the mean, variance, and covariance propagate through these two computations in Lemma 2 (dot product) and Lemma 3 (scalar GP gradient).

**Lemma 2.** Consider three Gaussian random vectors  $x, y, z$  with means  $\bar{x}, \bar{y}, \bar{z}$  and variances  $\text{Var}[x], \text{Var}[y], \text{Var}[z]$ , respectively. Let their pairwise covariances be  $\text{cov}(x, y)$ ,  $\text{cov}(y, z)$  and  $\text{cov}(z, x)$ . The mean, variance, and covariances of  $x^\top y$  are given by:

$$\mathbb{E}[x^\top y] = \bar{x}^\top \bar{y} + \frac{1}{2} \text{tr}(\text{cov}(x, y) + \text{cov}(y, x)) \quad (34)$$

$$\text{Var}[x^\top y] = \frac{1}{2} \text{tr}(\text{cov}(x, y) + \text{cov}(y, x))^2 + \bar{y}^\top \text{Var}[x] \bar{y} + \bar{x}^\top \text{Var}[y] \bar{x} + \bar{y}^\top \text{cov}(x, y) \bar{x} + \bar{x}^\top \text{cov}(y, x) \bar{y} \quad (35)$$

$$\begin{bmatrix} \text{cov}(x, x^\top y) \\ \text{cov}(y, x^\top y) \\ \text{cov}(z, x^\top y) \end{bmatrix} = \begin{bmatrix} \text{cov}(x, y) \bar{x} + \text{Var}[x] \bar{y} \\ \text{Var}[y] \bar{x} + \text{cov}(y, x) \bar{y} \\ \text{cov}(z, y) \bar{x} + \text{cov}(z, x) \bar{y} \end{bmatrix}. \quad (36)$$

*Proof.* See Appendix F.  $\square$

### Algorithm 1: Mean and variance of $\text{CBC}^{(2)}$ .

**Data:** ECBF  $h(x)$ , system dynamics distribution

$$\text{vec}(F(x)) \sim \mathcal{GP}(\text{vec}(M_k(x)), B_k(x, x') \otimes A)$$

**Result:**  $\mathbb{E}[\text{CBC}^{(2)}(x, u)]$  and  $\text{Var}[\text{CBC}^{(2)}(x, u)]$

- 1 Compute  $\mathbb{E}[\mathcal{L}_f h(x)] = \nabla_x h(x)^\top M_k(x) [1, 0_m^\top]^\top$  and  $\text{Var}[\mathcal{L}_f h(x)] = [B_k(x, x')]_{1,1} (\nabla_x h(x)^\top A \nabla_x h(x))$  by substituting  $\underline{u} = [1, 0_m^\top]^\top$  in Lemma 1.
- 2 Compute the mean and variance of  $\nabla_x \mathcal{L}_f h(x)$  using Lemma 3,
- 3 Compute  $\text{cov}(\nabla_x \mathcal{L}_f h(x), \mathcal{L}_f h(x))$  using (37)
- 4 Compute the mean and variance  $\nabla_x [\mathcal{L}_f h(x)]^\top F(x)\underline{u}$  using Lemma 2,
- 5 Compute  $\mathbf{d}(x)^\top \underline{u} = \text{cov}(\nabla_x [\mathcal{L}_f h(x)]^\top F(x)\underline{u}, \mathcal{L}_f h(x))$  using (36),
- 6 Plug the above values into (38) to obtain  $\mathbb{E}[\text{CBC}^{(2)}(x, u)]$  and  $\text{Var}[\text{CBC}^{(2)}(x, u)]$ .

**Lemma 3** ([93, Thm. 2.2.2][94, p. 43]). Let  $q(x)$  be a scalar Gaussian Process with differentiable mean function  $\mu(x) : \mathbb{R}^n \mapsto \mathbb{R}$  and twice-differentiable covariance function  $\kappa(x, x') : \mathbb{R}^n \times \mathbb{R}^n \mapsto \mathbb{R}$ . If  $\nabla_x \mu(x)$  exists and is finite for all  $x \in \mathbb{R}$  and  $\mathcal{H}_{x, x'} \kappa(x, x') = [\frac{\partial^2 \kappa(x, x')}{\partial x_i \partial x'_j}]_{i=1, j=1}^{n, n}$  exists and is finite for all  $(x, x') \in \mathbb{R}^{2n}$ , then  $q(x)$  possesses a mean square derivative  $\nabla_x q(x)$ , which is a vector-variate Gaussian Process  $\mathcal{GP}(\nabla_x \mu(x), \mathcal{H}_{x, x'} \kappa(x, x'))$ . If  $s$  is another random process whose finite covariance with  $q$  is  $\text{cov}_{q, s}(x, x')$ , then

$$\text{cov}(\nabla_x q(x), s(x')) = \nabla_x \text{cov}_{q, s}(x, x'). \quad (37)$$

We can compute the mean and variance of  $\text{CBC}^{(2)}$  for a relative degree two system using Proposition 7,

$$\begin{aligned} \mathbb{E}[\text{CBC}^{(2)}(x, u)] &= \mathbf{e}^{(2)}(x)^\top \underline{u} \\ \text{Var}[\text{CBC}^{(2)}(x, u)] &= \underline{u}^\top \mathbf{V}^{(2)}(x) \mathbf{V}^{(2)}(x)^\top \underline{u} \\ \mathbf{e}^{(2)}(x) &= \mathbb{E}[F(x)^\top \nabla_x \mathcal{L}_f h(x)] \\ &\quad + \begin{bmatrix} \mathbf{k}_{\alpha, 1} h(x) + \mathbf{k}_{\alpha, 2} \mathbb{E}[\mathcal{L}_f h(x)] \\ \mathbf{0}_m \end{bmatrix} \\ \mathbf{V}^{(2)}(x) &= \left( \text{Var}[F(x)^\top \nabla_x \mathcal{L}_f h(x)] \right. \\ &\quad \left. + \begin{bmatrix} \mathbf{k}_{\alpha, 2}^\top \text{Var}[\mathcal{L}_f h(x)] + 2[\mathbf{d}(x)]_1 & [\mathbf{d}(x)]_{2:m+1}^\top \\ [\mathbf{d}(x)]_{2:m+1} & \mathbf{0}_{m \times m} \end{bmatrix} \right)^{\frac{1}{2}} \\ \mathbf{d}(x) &\triangleq \mathbf{k}_{\alpha, 2} \text{cov}(F(x)^\top \nabla_x \mathcal{L}_f h(x), \mathcal{L}_f h(x)) \end{aligned} \quad (38)$$

where the terms in the above equations — the means, variances, and covariances of  $\mathcal{L}_f h(x)$  and  $F(x)^\top \nabla_x \mathcal{L}_f h(x)$  — can be computed via Algorithm 1 using Lemma 2 and Lemma 3.

## VIII. SIMULATIONS

We evaluate our proposed MVGP learning model as well as the SOCP-based safe control synthesis on two simulated systems: (A) Pendulum and (B) Ackermann Vehicle. To allow



reproducing the results, our implementation is available on Github<sup>3</sup>.

### A. Pendulum

Consider a pendulum, shown in Fig 5, with state  $\mathbf{x} = [\theta, \omega]^\top$ , containing its angular deviation  $\theta$  from the rest position and its angular velocity  $\omega$ . The pendulum dynamics are:

$$\begin{bmatrix} \dot{\theta} \\ \dot{\omega} \end{bmatrix} = \underbrace{\begin{bmatrix} \omega \\ -\frac{g}{l} \sin(\theta) \end{bmatrix}}_{f(\mathbf{x})} + \underbrace{\begin{bmatrix} 0 \\ \frac{1}{ml} \end{bmatrix}}_{g(\mathbf{x})} u, \quad (39)$$

where  $g$  is the gravitational acceleration,  $m$  is the mass, and  $l$  is the length.

1) *Estimating Pendulum Dynamics*: We compare our MVGP model versus the Coregionalization GP (CoGP) [71] in estimating the pendulum dynamics using data from randomly generated control inputs. In our simulation, the true pendulum model has mass  $m = 1$  and length  $l = 1$ . The inference algorithms were implemented in Python using GPyTorch [95]. We let  $\mathbf{K}_0(\mathbf{x}, \mathbf{x}') = \mathbf{B}\kappa_0(\mathbf{x}, \mathbf{x}') \otimes \mathbf{A}$  for MVGP and  $\mathbf{K}_0(\mathbf{x}, \mathbf{x}') = \Sigma\kappa_0(\mathbf{x}, \mathbf{x}')$  for CoGP, where  $\kappa_0(\mathbf{x}, \mathbf{x}')$  is a scaled radial-basis function kernel. Further,  $\mathbf{A}$ ,  $\mathbf{B}$ , and  $\Sigma$  are constrained to be positive semi-definite by modeling each as  $\mathbf{C}_r \mathbf{C}_r^\top + \text{diag}(\mathbf{v})$ , where  $\mathbf{C}_r \in \mathbb{R}^{l \times r}$ ,  $r$  is a desired rank and  $\text{diag}(\mathbf{v})$  is a diagonal matrix constructed from a vector  $\mathbf{v}$ .

We emphasize that a straightforward implementation of decoupled GPs for each system dimension is not possible because the training data is only available as a linear combination of the unknown functions  $f(\mathbf{x})$  and  $g(\mathbf{x})$ . We approximate decoupled GP inference by constraining the matrices  $\mathbf{A}$ ,  $\mathbf{B}$ , and  $\Sigma$  in the MVGP and CoGP models to be diagonal. To compare the accuracy of the GP models, we randomly split the samples from the pendulum simulation into training data and test data. Given a test set  $\mathcal{T}$ , we compute *variance-weighted error* as,

$$\text{err}(\mathcal{T}) \triangleq \sqrt{\sum_{\mathbf{x} \in \mathcal{T}} \frac{\|\mathbf{K}_k^{-\frac{1}{2}}(\mathbf{x}, \mathbf{x}) \text{vec}(\mathbf{M}_k(\mathbf{x}) - F(\mathbf{x}))\|_2^2}{|\mathcal{T}|}}. \quad (40)$$

A qualitative comparison of MVGP and CoGP is shown in Fig. 3. A quantitative comparison of the computational efficiency and inference accuracy of the models with *full* and *diagonal* covariance matrices is shown in Fig. 4. The median variance-weighted error and error bars showing the 2nd to 9th decile over 30 repetitions of the evaluation are shown. The experiments are performed on a desktop with Nvidia® GeForce RTX™ 2080Ti GPU and Intel® Core™ i9-7900X CPU (3.30GHz). The results show that MVGP inference is significantly faster than CoGP, while maintaining comparable accuracy. Both MVGP and CoGP have higher median accuracy than their counterparts with diagonally restricted covariances.

2) *Safe Control of Learned Pendulum Dynamics*: A safe set is chosen as the complement of a radial region  $[\theta_c - \Delta_{col}, \theta_c + \Delta_{col}]$  with  $\theta_c = 45^\circ$ ,  $\Delta_{col} = 22.5^\circ$  that needs to be avoided, as shown in Fig. 5. The control barrier function

defining this safe set is  $h(\mathbf{x}) = \cos(\Delta_{col}) - \cos(\theta - \theta_c)$ . The controller knows a priori that the system is control-affine with relative degree two, but it is not aware of  $f$  and  $g$ . A zero-mean prior  $\mathbf{M}_0(\mathbf{x}) = \mathbf{0}_{n \times (1+m)}$  and randomly generated covariance matrices  $\mathbf{A}$  and  $\mathbf{B}$  are used to initialize the MVGP model. We formulate a SOCP as in (30) with  $r = 2$ . We specify a task requiring the pendulum to track a reference control signal  $\hat{\pi}_k(\mathbf{x})$  and specify the optimization objective as  $\|\mathbf{R}(\mathbf{x}_k)(\mathbf{u}_k - \hat{\pi}_k(\mathbf{x}_k))\|_2^2$  with  $\mathbf{R}(\mathbf{x}_k) \equiv \mathbf{I}$ . The reference signal  $\hat{\pi}_k(\mathbf{x})$  is an  $\epsilon$ -greedy policy [96], used to provide sufficient excitation in the training data. Concretely,  $\hat{\pi}_k(\mathbf{x})$  is sampled from an  $\epsilon_k$  weighted combination of Dirac delta distribution  $\delta$  and Uniform distribution  $\mathbb{U}$ ,  $\hat{\pi}_k(\mathbf{x}_k) \sim (1 - \epsilon_k)\delta_{\mathbf{u}=0} + \epsilon_k\mathbb{U}[-20, 20]$ , where  $\epsilon_k = 10^{-k/50}$  so that  $\epsilon_k$  goes from 1 to 0.01 in 100 steps. We initialize the system with parameters  $\theta_0 = 75^\circ$ ,  $\omega_0 = -0.01$ ,  $\tau = 0.01$ ,  $m = 1$ ,  $g = 10$ ,  $l = 1$ . Our simulation results show that the pendulum remains in the safe region (see Fig. 5). Negative control inputs get rejected by the SOCP safety constraint, while positive inputs allow the pendulum to bounce back from the unsafe region.

### B. Ackermann Vehicle

Consider an Ackermann-drive vehicle model with state  $\mathbf{x} = [x, y, \theta]^\top$ , including position  $(x, y)$  and orientation  $\theta$ . To make the Ackermann dynamics affine in the control input, we define  $z \triangleq v \tan(\phi)$ , where  $v$  is the linear velocity and  $\phi$  is the steering angle. The Ackermann-drive dynamics are:

$$\begin{bmatrix} \dot{x} \\ \dot{y} \\ \dot{\theta} \end{bmatrix} = \underbrace{\begin{bmatrix} 0 \\ 0 \\ 0 \end{bmatrix}}_{f(\mathbf{x})} + \underbrace{\begin{bmatrix} \cos(\theta) & 0 \\ \sin(\theta) & 0 \\ 0 & \frac{1}{L} \end{bmatrix}}_{g(\mathbf{x})} \underbrace{\begin{bmatrix} v \\ z \end{bmatrix}}_{\mathbf{u}}, \quad (41)$$

where  $L$  is the distance between the front and back wheels.

a) *Estimating Ackermann-drive Dynamics*: Similar to Sec. VIII-A1, we compare the computational efficiency and inference accuracy of MVGP and CoGP with *diagonal* and *full* covariance matrices on training data generated from the Ackermann-drive model in (41). We further explicitly assume translation-invariant dynamics, i.e.,  $F(\mathbf{x}) = F([0, 0, \theta]^\top)$ ,  $\forall \mathbf{x} \in \mathbb{R}^3$ . This assumption allows us to transfer the learned dynamics to unvisited parts of the environment. The results of the simulation are shown in Fig. 4. We again find that MVGP inference is significantly faster than CoGP. In terms of accuracy, MVGP is comparable to CoGP and restricting the covariance matrices to diagonal matrices increases the median variance-weighted error.

b) *Safe Control of Learned Ackermann-drive Dynamics*: To test our safe controller on the Ackermann-drive vehicle, we consider navigation to a goal state in the presence of two circular obstacles in the environment. The CBF for circular obstacle  $i \in \{1, 2\}$  with center  $\mathbf{o}_i \in \mathbb{R}^2$  and radius  $r_i > 0$  is:

$$h_i(\mathbf{x}) = q_1(\|\mathbf{x}_{1:2} - \mathbf{o}_i\|_2^2 - r_i^2) + q_2 \cos(\theta - \phi_o), \quad (42)$$

where  $\phi_o = \tan^{-1}\left(\frac{y - \mathbf{o}_{i,2}}{x - \mathbf{o}_{i,1}}\right)$ . We assume that a planning algorithm provides a desired time-parameterized trajectory

<sup>3</sup>[https://github.com/wecacuee/Bayesian\\_CBF](https://github.com/wecacuee/Bayesian_CBF)

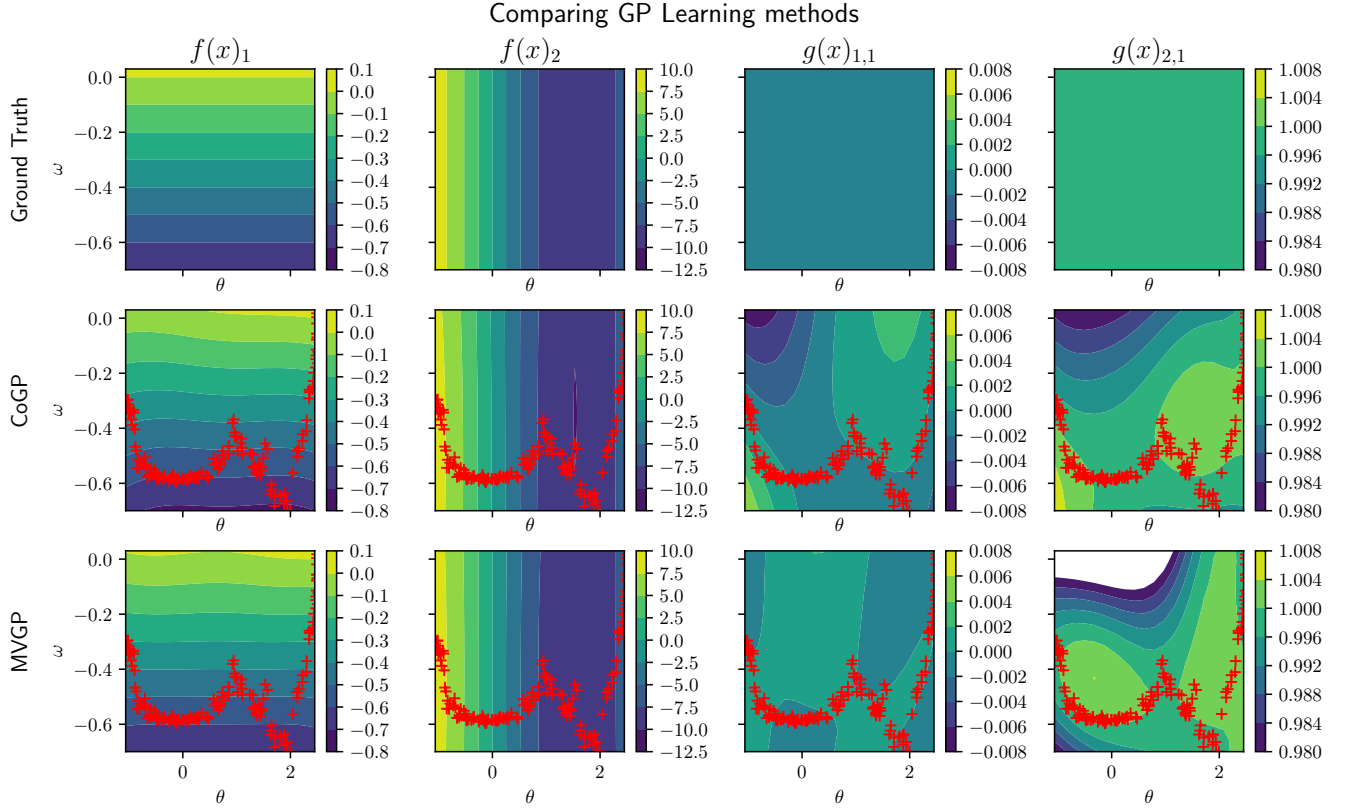


Fig. 3. Qualitative comparison of our Matrix Variate Gaussian Process (MVGP) regression with the Coregionalization GP (CoGP) model [71]. Training sample are generated using random control inputs to the pendulum. The training samples are shown as  $+$ . The learned models are evaluated on a  $20 \times 20$  grid, shown as contour plots. The MVGP model has lower computational complexity than CoGP ( $O(k^3)$  vs  $O(k^3 n^3)$ , see Sec. IV) without significant drop in accuracy.

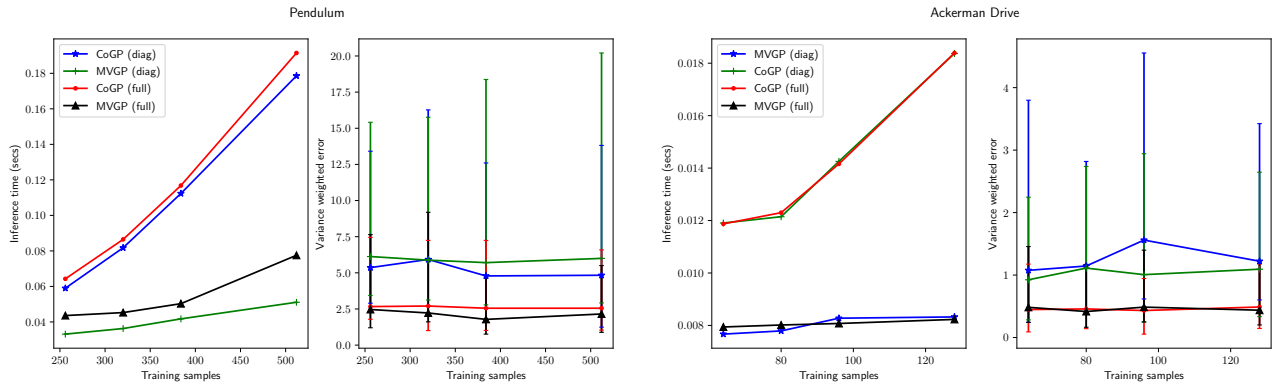


Fig. 4. Comparison of the computational efficiency and inference accuracy of MVGP and CoGP [71]. Both models are evaluated on the Pendulum and Ackerman systems in two modes: 1) with correlation matrix constrained to be diagonal (labelled *diag*) and 2) without any constraint on correlation matrix (labelled *full*). The results show that MVGP is significantly faster than CoGP. We argue in Sec. IV that the computational complexity of MVGP is  $O(k^3)$  for  $k$  training examples, while that of CoGP is  $O(k^3 n^3)$ , where  $n$  is the state dimension. The variance-weighted error is computed via (40). The error bars denote the range from the 2nd to the 9th decile over 30 repetitions, centered around the median. The median errors of the MVGP and CoGP models are similar but enforcing diagonal covariance matrices, increases the median error.

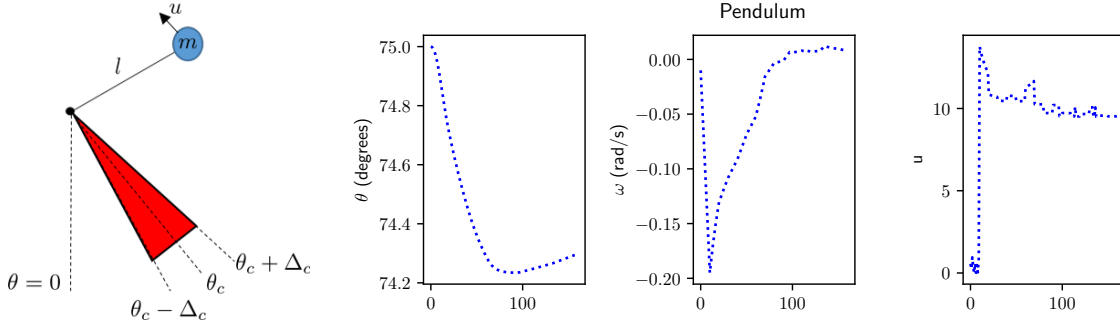


Fig. 5. Pendulum simulation (left) with an unsafe (red) region. The pendulum trajectory (middle two) resulting from the application of safe control inputs (right) is shown. The pendulum starts from  $\theta = 75^\circ$ , drops down until it reaches the unsafe region and then stays there.

$\mathbf{x}^{(d)} = [x^{(d)}, y^{(d)}, \theta^{(d)}]$  and its time derivative  $\dot{\mathbf{x}}^{(d)}$ . We select a control Lyapunov function candidate:

$$V(\mathbf{x}, \mathbf{x}^{(d)}) = \frac{w_1}{2} \rho^2 + w_2(1 - \cos(\alpha)), \quad (43)$$

where  $\rho \triangleq \|\mathbf{x}_{1:2}^{(d)} - \mathbf{x}_{1:2}\|_2$  and  $\alpha \triangleq \theta - \tan^{-1}\left(\frac{y^{(d)} - y}{x^{(d)} - x}\right)$ . The control Lyapunov condition is given by:

$$\text{CLC}(\mathbf{x}, \mathbf{u}) = \nabla_{\mathbf{x}}^\top V(\mathbf{x}, \mathbf{x}^{(d)}) F(\mathbf{x}) \mathbf{u} + \nabla_{\mathbf{x}^{(d)}}^\top V(\mathbf{x}, \mathbf{x}^{(d)}) \dot{\mathbf{x}}^{(d)} + \gamma_v V(\mathbf{x}, \mathbf{x}^{(d)}), \quad (44)$$

where

$$\nabla_{\mathbf{x}} V(\mathbf{x}, \mathbf{x}^{(d)}) = \begin{bmatrix} -w_1(x^{(d)} - x) - \frac{w_2}{\rho^2} \sin(\alpha)(y^{(d)} - y) \\ -w_1(y^{(d)} - y) + \frac{w_2}{\rho^2} \sin(\alpha)(x^{(d)} - x) \\ w_2 \sin(\alpha) \end{bmatrix}$$

$$\nabla_{\mathbf{x}^{(d)}} V(\mathbf{x}, \mathbf{x}^{(d)}) = \begin{bmatrix} w_1(x^{(d)} - x) + \frac{w_2}{\rho^2} \sin(\alpha)(y^{(d)} - y) \\ w_1(y^{(d)} - y) - \frac{w_2}{\rho^2} \sin(\alpha)(x^{(d)} - x) \\ 0 \end{bmatrix}.$$

The control Barrier condition for each obstacle  $i$  is:

$$\text{CBC}(\mathbf{x}, \mathbf{u}; i) = \nabla_{\mathbf{x}}^\top h_i(\mathbf{x}) F(\mathbf{x}) \mathbf{u} + \gamma_{h_i} h_i(\mathbf{x}), \quad (45)$$

where

$$\nabla_{\mathbf{x}} h_i(\mathbf{x}) = \begin{bmatrix} 2q_1(x - \mathbf{o}_{i,0}) + \frac{q_2}{\rho_{o,i}^2}(\mathbf{o}_{i,1} - y) \sin(\phi_o - \theta) \\ 2q_1(y - \mathbf{o}_{i,1}) - \frac{q_2}{\rho_{o,i}^2}(\mathbf{o}_{i,0} - x) \sin(\phi_o - \theta) \\ -q_2 \sin(\theta - \phi_o) \end{bmatrix}.$$

We implement the SOCP controller in Prop. 4 with parameters:  $q_1 = 0.7$ ,  $q_2 = 0.3$ ,  $w_1 = 0.9$ ,  $w_2 = 1.5$ ,  $\gamma_{h_i} = 5$ ,  $\gamma_v = 10$ ,  $\tau = 0.01$ .

We perform two experiments to evaluate the advantages of our model. First, we evaluate the importance of *accounting for the variance* of the dynamics estimate for safe control. Second, we evaluate the importance of *online learning* in reducing the variance and ensuring safety.

Recall the observation in Prop. 4 that  $c(\tilde{p}_k = 0.5) = 0$ . In this case, the SOCP in (19) reduces to the deterministic-case QP in (4). We dub the case of  $\tilde{p}_k = 0.5$  as *Mean CBF* and the case of  $\tilde{p}_k = 0.99$  as *Bayes CBF*. In both the cases, the covariance matrices are initialized as  $\mathbf{A} = 0.01\mathbf{I}_3$  and  $\mathbf{B} = \mathbf{I}_3$ . The true dynamics,  $F(\mathbf{x})$ , is specified with  $L = 12$ , while the mean dynamics  $\mathbf{M}_0(\mathbf{x})$  is obtained with  $L = 1$ . The result of simulation is shown in Fig. 6. The *Bayes CBF* controller

slows down when the safety constraint in (19d) hits zero and then changes direction while avoiding the obstacle. However, the *Mean CBF* controller is not able to avoid the obstacle because it does not take the variance of the dynamics estimate into account and the mean dynamics are inaccurate.

We also evaluate the importance of *online learning* for safe control. We compare two setups: (1) updating the system dynamics estimate online via our MVGP approach every 40 steps using the data collected so far (*With Learning*) and (2) relying on the prior system dynamics estimate only (*No Learning*). In both the cases, we choose  $\tilde{p}_k = 0.99$ . The true dynamics are specified with  $L = 1$ , while prior mean dynamics correspond to  $L = 8$ . The covariance matrices  $\mathbf{A}$  and  $\mathbf{B}$  are initialized with elements independently sampled from a standard Gaussian distribution while ensuring them to positive semi-definite as before. The result are shown in Fig. 7. Online learning of the vehicle dynamics reduces the variance and allows the vehicle to pass between the two obstacles. This is not possible using the prior dynamics distribution because the large variance makes the safety constraint in (19d) conservative.

## IX. CONCLUSION

Allowing artificial systems to safely adapt their own models during online operation will have significant implications for their successful use in unstructured changing real-world environments. This paper developed a Bayesian inference approach to approximate system dynamics and their uncertainty from online observations. The posterior distribution over the dynamics was used to specify probabilistic constraints that guarantee safe and stable online operation with high probability. Our results offer a promising approach for controlling complex systems in challenging environments. Future work will focus on applications of the proposed approach to real robot systems.

## REFERENCES

- [1] M. J. Khojasteh, V. Dhiman, M. Franceschetti, and N. Atanasov, "Probabilistic Safety Constraints for Learned High Relative Degree System Dynamics," in *Learning for Dynamics and Control (L4DC)*, 2020.
- [2] K.-D. Kim and P. R. Kumar, "Cyber-physical systems: A perspective at the centennial," *Proceedings of the IEEE*, vol. 100, pp. 1287–1308, 2012.
- [3] R. M. Murray, K. J. Astrom, S. P. Boyd, R. W. Brockett, and G. Stein, "Future directions in control in an information-rich world," *IEEE Control Systems*, vol. 23, no. 2, pp. 20–33, 2003.

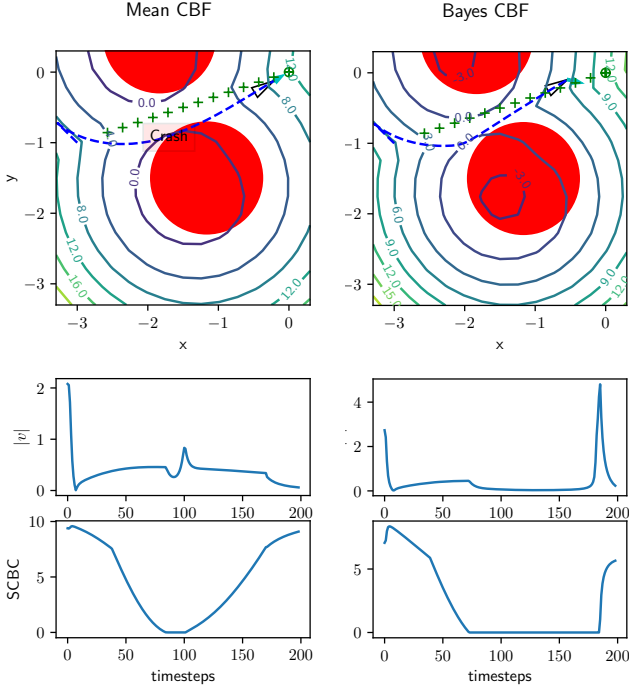


Fig. 6. Comparison of enforcing CBF constraints with Ackermann dynamics when accounting (*Bayes CBF*) and not accounting (*Mean CBF*) for the variance in the dynamics estimate. The top row shows the Ackermann vehicle trajectory in dashed blue with two obstacles in red, obtained The contour plots shows the minimum of the SCBC (19d) values corresponding to the two obstacles, evaluated on the  $(x, y)$  grid while keeping  $\theta$  and  $\mathbf{u}$  fixed. The middle row shows the magnitude of the velocity input over time. The bottom row shows the minimum of the two SCBC (19d) values over time. Enforcing safety using only the mean CBC (*Mean CBF*) results in a collision, while accounting for stochastic CBC (*Bayes CBF*) constraint causes the Ackermann vehicle to slow down and turn away from the unsafe region. A video rendering of these simulations is available in the supplementary material.

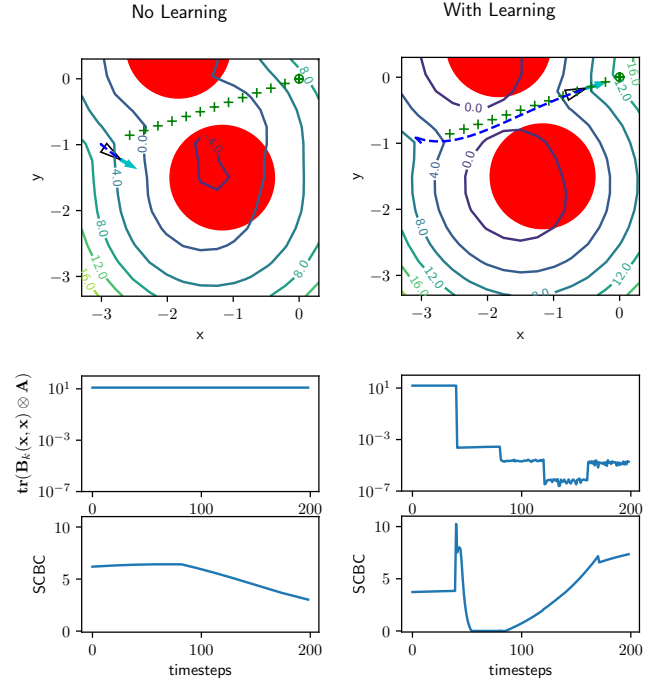


Fig. 7. The effect of online dynamics learning (right) versus no online learning (left) on the safe control of an Ackermann vehicle. The top row shows the vehicle trajectory in dashed blue with two obstacles in red. The middle row shows the trace of the covariance matrix  $\text{tr}(\mathbf{B}_k(\mathbf{x}, \mathbf{x}) \otimes \mathbf{A})$ , which we use as a measure of uncertainty. The bottom row shows the minimum of the two probabilistic safety constraint over time, as defined in (19d). Note that without learning, the vehicle gets stuck between the two obstacles because the uncertainty in the dynamics is too high, i.e., the safety condition in (19d) cannot be rendered positive. With online learning, however, the uncertainty is reduced enough to allow the safety condition to become positive in the area between the two obstacles. The dynamics distribution is updated every 40 time steps. Note the drop in uncertainty in the middle row at these time steps. A video rendering of these simulations is available in the supplementary material.

[4] J. A. Bagnell, D. Bradley, D. Silver, B. Sofman, and A. Stentz, "Learning for autonomous navigation," *IEEE Robotics & Automation Magazine*, vol. 17, no. 2, pp. 74–84, 2010.

[5] B. Thananjeyan, A. Balakrishna, U. Rosolia, F. Li, R. McAllister, J. E. Gonzalez, S. Levine, F. Borrelli, and K. Goldberg, "Safety Augmented Value Estimation from Demonstrations (SAVED): Safe Deep Model-Based RL for Sparse Cost Robotic Tasks," *IEEE Robotics and Automation Letters*, vol. 5, no. 2, pp. 3612–3619, 2020.

[6] M. Deisenroth and C. E. Rasmussen, "PILCO: A model-based and data-efficient approach to policy search," in *International Conference on machine learning (ICML)*, 2011, pp. 465–472.

[7] S. Dean, H. Mania, N. Matni, B. Recht, and S. Tu, "On the Sample Complexity of the Linear Quadratic Regulator," *Foundations of Computational Mathematics*, vol. 20, pp. 633–679, 2020.

[8] T. Sarkar and A. Rakhlin, "Near optimal finite time identification of arbitrary linear dynamical systems," in *International Conference on Machine Learning (ICML)*, 2019, pp. 5610–5618.

[9] J. Coulson, J. Lygeros, and F. Dörfler, "Data-enabled predictive control: in the shadows of the DeepPC," in *European Control Conference (ECC)*. IEEE, 2019, pp. 307–312.

[10] S. Chen, K. Saulnier, N. Atanasov, D. D. Lee, V. Kumar, G. J. Pappas, and M. Morari, "Approximating explicit model predictive control using constrained neural networks," in *American Control Conference (ACC)*. IEEE, 2018, pp. 1520–1527.

[11] M. J. Khojasteh, A. Khina, M. Franceschetti, and T. Javidi, "Learning-based Attacks in Cyber-Physical Systems," *IEEE Transactions on Control of Network Systems*, 2020.

[12] A. Liu, G. Shi, S.-J. Chung, A. Anandkumar, and Y. Yue, "Robust regression for safe exploration in control," in *Learning for Dynamics and Control (LADC)*, 2020, pp. 608–619.

[13] D. D. Fan, A.-a. Agha-mohammadi, and E. A. Theodorou, "Deep

Learning Tubes for Tube MPC," *Robotics: Science and Systems*, 2020.

[14] G. Chowdhary, H. A. Kingravi, J. P. How, and P. A. Vela, "Bayesian nonparametric adaptive control using Gaussian processes," *IEEE Transactions on Neural Networks and Learning Systems*, vol. 26, no. 3, pp. 537–550, 2014.

[15] A. Lakshmanan, A. Gahlawat, and N. Hovakimyan, "Safe feedback motion planning: A contraction theory and L1-adaptive control based approach," *arXiv preprint arXiv:2004.01142*, 2020.

[16] S. Levine, C. Finn, T. Darrell, and P. Abbeel, "End-to-end training of deep visuomotor policies," *The Journal of Machine Learning Research*, vol. 17, no. 1, pp. 1334–1373, 2016.

[17] Y. Pan, C.-A. Cheng, K. Saigol, K. Lee, X. Yan, E. Theodorou, and B. Boots, "Agile Autonomous Driving using End-to-End Deep Imitation Learning," in *Robotics: science and systems*, 2018.

[18] G. Kahn, P. Abbeel, and S. Levine, "BADGR: An autonomous self-supervised learning-based navigation system," *arXiv preprint arXiv:2002.05700*, 2020.

[19] M. Ono, B. Rothrock, K. Otsu, S. Higa, Y. Iwashita, A. Didier, T. Islam, C. Laporte, V. Sun, K. Stack *et al.*, "MAARS: Machine learning-based Analytics for Automated Rover Systems," in *Aerospace Conference*. IEEE, 2020, pp. 1–17.

[20] P. Wieland and F. Allgöwer, "Constructive safety using control barrier functions," *IFAC Proceedings Volumes*, vol. 40, no. 12, pp. 462–467, 2007.

[21] A. D. Ames, X. Xu, J. W. Grizzle, and P. Tabuada, "Control barrier function based quadratic programs for safety critical systems," *IEEE Transactions on Automatic Control*, vol. 62, no. 8, pp. 3861–3876, 2016.

[22] X. Xu, T. Waters, D. Pickem, P. Glotfelter, M. Egerstedt, P. Tabuada, J. W. Grizzle, and A. D. Ames, "Realizing simultaneous lane keeping and adaptive speed regulation on accessible mobile robot testbeds,"



- in *IEEE Conference on Control Technology and Applications (CCTA)*, 2017, pp. 1769–1775.
- [23] X. Xu, P. Tabuada, J. W. Grizzle, and A. D. Ames, “Robustness of control barrier functions for safety critical control,” *IFAC-PapersOnLine*, vol. 48, no. 27, pp. 54–61, 2015.
- [24] S. Prajna, A. Jadbabaie, and G. J. Pappas, “A framework for worst-case and stochastic safety verification using barrier certificates,” *IEEE Transactions on Automatic Control*, vol. 52, no. 8, pp. 1415–1428, 2007.
- [25] A. D. Ames, S. Coogan, M. Egerstedt, G. Notomista, K. Sreenath, and P. Tabuada, “Control Barrier Functions: Theory and Applications,” in *European Control Conference (ECC)*, June 2019, pp. 3420–3431.
- [26] F. S. Barbosa, L. Lindemann, D. V. Dimarogonas, and J. Tumova, “Provably Safe Control of Lagrangian Systems in Obstacle-Scattered Environments,” *arXiv preprint arXiv:2009.02148*, 2020.
- [27] M. Jankovic, “Robust control barrier functions for constrained stabilization of nonlinear systems,” *Automatica*, vol. 96, pp. 359–367, 2018.
- [28] L. Lindemann and D. V. Dimarogonas, “Control barrier functions for multi-agent systems under conflicting local signal temporal logic tasks,” *IEEE Control Systems Letters*, vol. 3, no. 3, pp. 757–762, 2019.
- [29] K. Garg and D. Panagou, “Control-lyapunov and control-barrier functions based quadratic program for spatio-temporal specifications,” in *Conference on Decision and Control (CDC)*. IEEE, 2019, pp. 1422–1429.
- [30] G. Yang, C. Belta, and R. Tron, “Self-triggered control for safety critical systems using control barrier functions,” in *American Control Conference (ACC)*. IEEE, 2019, pp. 4454–4459.
- [31] J. Umlauf and S. Hirche, “Feedback linearization based on gaussian processes with event-triggered online learning,” *IEEE Transactions on Automatic Control*, vol. 65, no. 10, pp. 4154–4169, 2020.
- [32] F. Solowjow and S. Trimpe, “Event-triggered learning,” *Automatica*, vol. 117, p. 109009, 2020.
- [33] W. Heemels, K. H. Johansson, and P. Tabuada, “An introduction to event-triggered and self-triggered control,” in *Conference on Decision and Control (CDC)*. IEEE, 2012, pp. 3270–3285.
- [34] K. Hashimoto, Y. Yoshimura, and T. Ushio, “Learning self-triggered controllers with Gaussian processes,” *IEEE Transactions on Cybernetics*, 2020, to appear.
- [35] S.-C. Hsu, X. Xu, and A. D. Ames, “Control barrier function based quadratic programs with application to bipedal robotic walking,” in *American Control Conference (ACC)*. IEEE, 2015, pp. 4542–4548.
- [36] Q. Nguyen and K. Sreenath, “Optimal robust control for constrained nonlinear hybrid systems with application to bipedal locomotion,” in *American Control Conference (ACC)*. IEEE, 2016, pp. 4807–4813.
- [37] Q. Nguyen and K. Sreenath, “Exponential Control Barrier Functions for enforcing high relative-degree safety-critical constraints,” in *American Control Conference (ACC)*. IEEE, 2016, pp. 322–328.
- [38] W. Xiao and C. Belta, “Control barrier functions for systems with high relative degree,” in *Conference on Decision and Control (CDC)*. IEEE, 2019, pp. 474–479.
- [39] T. Koller, F. Berkenkamp, M. Turchetta, and A. Krause, “Learning-based model predictive control for safe exploration,” in *Conference on Decision and Control (CDC)*. IEEE, 2018, pp. 6059–6066.
- [40] F. Berkenkamp, A. P. Schoellig, and A. Krause, “Safe controller optimization for quadrotors with Gaussian processes,” in *International Conference on Robotics and Automation (ICRA)*, 2016, pp. 493–496.
- [41] J. F. Fisac, A. K. Akametalu, M. N. Zeilinger, S. Kaynama, J. Gillula, and C. J. Tomlin, “A general safety framework for learning-based control in uncertain robotic systems,” *IEEE Transactions on Automatic Control*, vol. 64, no. 7, pp. 2737–2752, 2018.
- [42] O. Bastani, “Safe Reinforcement Learning with Nonlinear Dynamics via Model Predictive Shielding,” *arXiv preprint arXiv:1905.10691*, 2019.
- [43] K. P. Wabersich and M. N. Zeilinger, “Safe exploration of nonlinear dynamical systems: A predictive safety filter for reinforcement learning,” *arXiv preprint arXiv:1812.05506*, 2018.
- [44] E. Biyik, J. Margoliash, S. R. Alimo, and D. Sadigh, “Efficient and safe exploration in deterministic markov decision processes with unknown transition models,” in *American Control Conference (ACC)*. IEEE, 2019, pp. 1792–1799.
- [45] N. Jansen, B. Könighofer, S. Junges, and R. Bloem, “Shielded decision-making in MDPs,” *arXiv preprint arXiv:1807.06096*, 2018.
- [46] T. Lew, R. Bonalli, and M. Pavone, “Chance-constrained sequential convex programming for robust trajectory optimization,” in *European Control Conference (ECC)*. IEEE, 2020, pp. 1871–1878.
- [47] A. Clark, “Control Barrier Functions for Complete and Incomplete Information Stochastic Systems,” in *American Control Conference (ACC)*. IEEE, 2019, pp. 2928–2935.
- [48] C. Santoyo, M. Dutreix, and S. Coogan, “A Barrier Function Approach to Finite-Time Stochastic System Verification and Control,” *Automatica*, 2020.
- [49] M. Aloysius Pereira, Z. Wang, I. Exarchos, and E. A. Theodorou, “Safe Optimal Control Using Stochastic Barrier Functions and Deep Forward-Backward SDEs,” *arXiv preprint arXiv:2009.01196*, 2020.
- [50] D. D. Fan, J. Nguyen, R. Thakker, N. Alatur, A. a. Agha-mohammadi, and E. A. Theodorou, “Bayesian Learning-Based Adaptive Control for Safety Critical Systems,” in *IEEE International Conference on Robotics and Automation (ICRA)*, 2020, pp. 4093–4099.
- [51] L. Wang, E. A. Theodorou, and M. Egerstedt, “Safe learning of quadrotor dynamics using barrier certificates,” in *International Conference on Robotics and Automation (ICRA)*. IEEE, 2018, pp. 2460–2465.
- [52] R. Cheng, G. Orosz, R. M. Murray, and J. W. Burdick, “End-to-end safe reinforcement learning through barrier functions for safety-critical continuous control tasks,” in *AAAI Conference on Artificial Intelligence*, vol. 33, 2019, pp. 3387–3395.
- [53] Z. Marvi and B. Kiumarsi, “Safe Off-policy Reinforcement Learning Using Barrier Functions,” in *American Control Conference (ACC)*. IEEE, 2020, pp. 2176–2181.
- [54] A. J. Taylor and A. D. Ames, “Adaptive Safety with Control Barrier Functions,” in *American Control Conference (ACC)*, 2020, pp. 1399–1405.
- [55] B. T. Lopez, J.-J. E. Slotine, and J. P. How, “Robust Adaptive Control Barrier Functions: An Adaptive and Data-Driven Approach to Safety,” *IEEE Control Systems Letters*, vol. 5, no. 3, pp. 1031–1036, 2020.
- [56] I. Salehi, G. Yao, and A. P. Dani, “Active Sampling based Safe Identification of Dynamical Systems using Extreme Learning Machines and Barrier Certificates,” in *IEEE International Conference on Robotics and Automation (ICRA)*, 2019, pp. 22–28.
- [57] A. Taylor, A. Singletary, Y. Yue, and A. Ames, “Learning for safety-critical control with control barrier functions,” in *Learning for Dynamics and Control (L4DC)*, 2020, pp. 708–717.
- [58] C. K. Williams and C. E. Rasmussen, *Gaussian processes for machine learning*. MIT press Cambridge, MA, 2006, vol. 2, no. 3.
- [59] Y. Gal and Z. Ghahramani, “Dropout as a Bayesian approximation: Representing model uncertainty in deep learning,” in *International Conference on Machine Learning*, 2016, pp. 1050–1059.
- [60] J. Harrison, A. Sharma, and M. Pavone, “Meta-learning Priors for Efficient Online Bayesian Regression,” in *Workshop on the Algorithmic Foundations of Robotics*. Springer, 2018, pp. 318–337.
- [61] B. Efron and T. Hastie, *Computer age statistical inference*. Cambridge University Press, 2016, vol. 5.
- [62] F. Berkenkamp, M. Turchetta, A. Schoellig, and A. Krause, “Safe model-based reinforcement learning with stability guarantees,” in *Advances in Neural Information Processing Systems*, 2017, pp. 908–918.
- [63] P. Jagtap, G. J. Pappas, and M. Zamani, “Control Barrier Functions for Unknown Nonlinear Systems using Gaussian Processes,” in *IEEE Conference on Decision and Control (CDC)*, 2020.
- [64] U. Rosolia and A. D. Ames, “Multi-Rate Control Design Leveraging Control Barrier Functions and Model Predictive Control Policies,” *IEEE Control Systems Letters*, 2020.
- [65] X. Da, Z. Xie, D. Hoeller, B. Boots, A. Anandkumar, Y. Zhu, B. Babich, and A. Garg, “Learning a Contact-Adaptive Controller for Robust, Efficient Legged Locomotion,” *arXiv preprint arXiv:2009.10019*, 2020.
- [66] S. Singh, A. Majumdar, J.-J. Slotine, and M. Pavone, “Robust online motion planning via contraction theory and convex optimization,” in *International Conference on Robotics and Automation (ICRA)*. IEEE, 2017, pp. 5883–5890.
- [67] B. T. Lopez and J. E. Slotine, “Adaptive Nonlinear Control With Contraction Metrics,” *IEEE Control Systems Letters*, vol. 5, no. 1, pp. 205–210, 2021.
- [68] K. Lowrey, A. Rajeswaran, S. Kakade, E. Todorov, and I. Mordatch, “Plan Online, Learn Offline: Efficient Learning and Exploration via Model-Based Control,” in *International Conference on Learning Representations*, 2019.
- [69] D. Sun, S. Jha, and C. Fan, “Learning Certified Control using Contraction Metric,” in *Conference on Robot Learning (CoRL)*, 2020.
- [70] H. Tsukamoto and S. J. Chung, “Robust controller design for stochastic nonlinear systems via convex optimization,” *IEEE Transactions on Automatic Control*, 2020, to appear.
- [71] M. A. Alvarez, L. Rosasco, and N. D. Lawrence, “Kernels for vector-valued functions: A review,” *Foundations and Trends in Machine Learning*, vol. 4, no. 3, pp. 195–266, 2012.
- [72] S. Sun, C. Chen, and L. Carin, “Learning Structured Weight Uncertainty in Bayesian Neural Networks,” in *International Conference on Artificial Intelligence and Statistics (AISTATS)*, 2017, pp. 1283–1292.

- [73] C. Louizos and M. Welling, "Structured and efficient variational deep learning with matrix Gaussian posteriors," in *International Conference on Machine Learning*, 2016, pp. 1708–1716.
- [74] S. Ghosal and A. Roy, "Posterior consistency of Gaussian process prior for nonparametric binary regression," *The Annals of Statistics*, vol. 34, no. 5, pp. 2413–2429, 2006.
- [75] S. Shekhar and T. Javidi, "Gaussian process bandits with adaptive discretization," *Electronic Journal of Statistics*, vol. 12, no. 2, pp. 3829–3874, 2018.
- [76] N. Srinivas, A. Krause, S. M. Kakade, and M. Seeger, "Gaussian process optimization in the bandit setting: no regret and experimental design," in *International Conference on Machine Learning*, 2010.
- [77] A. Lederer, J. Umlauft, and S. Hirche, "Uniform error bounds for Gaussian process regression with application to safe control," in *Advances in Neural Information Processing Systems*, 2019, pp. 659–669.
- [78] M. S. Lobo, L. Vandenberghe, S. Boyd, and H. Lebre, "Applications of second-order cone programming," *Linear algebra and its applications*, vol. 284, no. 1-3, pp. 193–228, 1998.
- [79] Gurobi Optimization, LLC, "Gurobi Optimizer Reference Manual," Online: <http://www.gurobi.com>, 2020.
- [80] L. Vandenberghe, "The CVXOPT linear and quadratic cone program solvers," Online: <https://cvxopt.org/userguide/coneprog>, 2010.
- [81] A. Lederer, J. Umlauft, and S. Hirche, "Posterior variance analysis of Gaussian processes with application to average learning curves," *arXiv preprint arXiv:1906.01404*, 2019.
- [82] Y. K. Nakka, A. Liu, G. Shi, A. Anandkumar, Y. Yue, and S.-J. Chung, "Chance-Constrained Trajectory Optimization for Safe Exploration and Learning of Nonlinear Systems," *IEEE Robotics and Automation Letters*, 2020, to appear.
- [83] T. Lew, A. Sharma, J. Harrison, and M. Pavone, "Safe Model-Based Meta-Reinforcement Learning: A Sequential Exploration-Exploitation Framework," *arXiv preprint arXiv:2008.11700*, 2020.
- [84] E. Schmerling and M. Pavone, "Evaluating trajectory collision probability through adaptive importance sampling for safe motion planning," in *Robotics: Science and Systems*, 2017.
- [85] K. Oguri, M. Ono, and J. W. McMahon, "Convex Optimization over Sequential Linear Feedback Policies with Continuous-time Chance Constraints," in *Conference on Decision and Control (CDC)*. IEEE, 2019, pp. 6325–6331.
- [86] G. Yang, B. Vang, Z. Serlin, C. Belta, and R. Tron, "Sampling-based Motion Planning via Control Barrier Functions," in *International Conference on Automation, Control and Robots*, 2019, pp. 22–29.
- [87] P. Akella, M. Ahmadi, R. M. Murray, and A. D. Ames, "Formal Test Synthesis for Safety-Critical Autonomous Systems based on Control Barrier Functions," *arXiv preprint arXiv:2004.04227*, 2020.
- [88] A. Robey, H. Hu, L. Lindemann, H. Zhang, D. V. Dimarogonas, S. Tu, and N. Matni, "Learning Control Barrier Functions from Expert Demonstrations," *arXiv preprint arXiv:2004.03315*, 2020.
- [89] M. Srinivasan, A. Dabholkar, S. Coogan, and P. Vela, "Synthesis of control barrier functions using a supervised machine learning approach," *International Conference on Intelligent Robots and Systems*, 2020.
- [90] W. Xiao, C. Belta, and C. G. Cassandras, "Adaptive Control Barrier Functions for Safety-Critical Systems," *arXiv preprint arXiv:2002.04577*, 2020.
- [91] M. Sarkar, D. Ghose, and E. A. Theodorou, "High-Relative Degree Stochastic Control Lyapunov and Barrier Functions," *arXiv preprint arXiv:2004.03856*, 2020.
- [92] S. Yaghoubi, G. Fainekos, and S. Sankaranarayanan, "Training neural network controllers using control barrier functions in the presence of disturbances," *arXiv preprint arXiv:2001.08088*, 2020.
- [93] R. J. Adler, *The geometry of random fields*. Chichester : John Wiley and Sons, 1981.
- [94] J. Taylor, "STAT352, Spatial Statistics: Notes on Random Fields," Stanford University, [http://statweb.stanford.edu/~jtaylo/courses/stats352/notes/random\\_fields.pdf](http://statweb.stanford.edu/~jtaylo/courses/stats352/notes/random_fields.pdf), 2009.
- [95] J. R. Gardner, G. Pleiss, D. Bindel, K. Q. Weinberger, and A. G. Wilson, "GPpyTorch: Blackbox Matrix-Matrix Gaussian Process Inference with GPU Acceleration," in *Advances in Neural Information Processing Systems*, 2018.
- [96] R. S. Sutton and A. G. Barto, *Reinforcement learning: An introduction*. MIT press, 2018.
- [97] S. R. Searle and M. H. Gruber, *Linear models*. John Wiley & Sons, 1971.



**Vikas Dhiman** is a Postdoctoral Researcher at the Contextual Robotics Institute and the Existential Robotics Lab at the University of California, San Diego. His works lie in the localization, mapping and control algorithms for applications in robotics. He graduated in Elec. Engg (2008) from Indian Institute of Technology, Roorkee, earned his MS (2014) from University at Buffalo, and received his PhD (2019) from the University of Michigan, Ann Arbor.



**Mohammad Javad Khojasteh** (S'14–M'21) did his undergraduate studies at Sharif University of Technology from which he received double-major B.Sc. degrees in Electrical Engineering and in Pure Mathematics, in 2015. He received the M.Sc. and Ph.D. degrees in Electrical and Computer Engineering from University of California San Diego (UCSD), La Jolla, CA, in 2017, and 2019, respectively. From January 2020 to October 2020, he was a postdoctoral scholar with Center for Autonomous Systems and Technology (CAST) at California Institute of Technology (Caltech), and a visitor at NASA's Jet Propulsion Laboratory (JPL), where he worked with Team CoSTAR. Currently, he is a Postdoctoral Scholar at Massachusetts Institute of Technology (MIT).



**Massimo Franceschetti** (M'98–SM'11–F'18) received the Laurea degree (with highest honors) in computer engineering from the University of Naples, Naples, Italy, in 1997, the M.S. and Ph.D. degrees in electrical engineering from the California Institute of Technology, in 1999, and 2003, respectively. He is Professor of Electrical and Computer Engineering at the University of California at San Diego (UCSD). Before joining UCSD, he was a postdoctoral scholar at the University of California at Berkeley for two years. He has held visiting positions at the Vrije Universiteit Amsterdam, the École Polytechnique Fédérale de Lausanne, and the University of Trento. His research interests are in physical and information-based foundations of communication and control systems. He was awarded the C. H. Wilts Prize in 2003 for best doctoral thesis in electrical engineering at Caltech; the S.A. Schelkunoff Award in 2005 for best paper in the IEEE Transactions on Antennas and Propagation, a National Science Foundation (NSF) CAREER award in 2006, an Office of Naval Research (ONR) Young Investigator Award in 2007, the IEEE Communications Society Best Tutorial Paper Award in 2010, and the IEEE Control theory society Ruberti young researcher award in 2012. He has been elected fellow of the IEEE in 2018 and became a Guggenheim fellow for the natural sciences: engineering in 2019.



**Nikolay Atanasov** (S'07–M'16) is an Assistant Professor of Electrical and Computer Engineering at the University of California San Diego. He obtained a B.S. degree in Electrical Engineering from Trinity College, Hartford, CT, in 2008 and M.S. and Ph.D. degrees in Electrical and Systems Engineering from the University of Pennsylvania, Philadelphia, PA, in 2012 and 2015, respectively. His research focuses on robotics, control theory, and machine learning, applied to active sensing using ground and aerial robots. He works on probabilistic environment models that unify geometry and semantics and on optimal control and reinforcement learning approaches for minimizing uncertainty in these models. Dr. Atanasov's work has been recognized by the Joseph and Rosaline Wolf award for the best Ph.D. dissertation in Electrical and Systems Engineering at the University of Pennsylvania in 2015 and the best conference paper award at the International Conference on Robotics and Automation in 2017.

## APPENDIX A

## ADDITIONAL PROPERTIES OF THE MVG DISTRIBUTION

**Lemma 4** ([72]). Let  $\mathbf{X}$  follow an MVG distribution  $\mathcal{MN}(\mathbf{M}, \mathbf{A}, \mathbf{B})$ . Then,  $\text{vec}(\mathbf{X}) \sim \mathcal{N}(\text{vec}(\mathbf{M}), \mathbf{B} \otimes \mathbf{A})$ .

**Lemma 5** ([72]). Let  $\mathbf{X}$  follow an MVG distribution  $\mathcal{MN}(\mathbf{M}, \mathbf{A}, \mathbf{B})$  and let  $\mathbf{C} \in \mathbb{R}^{d \times n}$  and  $\mathbf{D} \in \mathbb{R}^{m \times d}$ . Then,

$$\begin{aligned} \mathbf{CX} &\sim \mathcal{MN}(\mathbf{CM}, \mathbf{CAC}^\top, \mathbf{B}), \\ \mathbf{XD} &\sim \mathcal{MN}(\mathbf{MD}, \mathbf{A}, \mathbf{D}^\top \mathbf{BD}), \end{aligned} \quad (46)$$

## APPENDIX B

## PROOF OF PROPOSITION 3

Let  $\mathcal{GP}(\text{vec}(\mathbf{M}_k(\mathbf{x})), \mathbf{K}_k(\mathbf{x}, \mathbf{x}'))$  be the posterior distribution of  $\text{vec}(F(\mathbf{x}))$  conditioned on the training data  $(\mathbf{X}_{1:k}, \mathbf{U}_{1:k}, \mathbf{X}_{1:k})$ . The mean and variance can be obtained by applying Schur's complement to (8),

$$\text{vec}(\mathbf{M}_k(\mathbf{x})) = \text{vec}(\mathbf{M}_0(\mathbf{x})) + \quad (47)$$

$$\begin{aligned} &(\mathbf{B}_{1:k}(\mathbf{x}) \otimes \mathbf{A})^\top (\mathbf{B}_{1:k}^{1:k} \otimes \mathbf{A})^{-1} \text{vec}(\mathbf{X} - \mathbf{M}_{1:k} \mathbf{U}_{1:k}), \\ \mathbf{K}_k(\mathbf{x}, \mathbf{x}) &= \mathbf{B}_0(\mathbf{x}, \mathbf{x}) \otimes \mathbf{A} - \quad (48) \\ &(\mathbf{B}_{1:k}(\mathbf{x}) \otimes \mathbf{A})^\top (\mathbf{B}_{1:k}^{1:k} \otimes \mathbf{A})^{-1} (\mathbf{B}_{1:k}^\top(\mathbf{x}) \otimes \mathbf{A}). \end{aligned}$$

where  $\mathbf{B}_{1:k}^{1:k} \triangleq \mathbf{U}_{1:k}^\top \mathbf{B}_{1:k} \mathbf{U}_{1:k} + \sigma^2 \mathbf{I}_k$  and  $\mathbf{B}_{1:k}(\mathbf{x}) \triangleq \mathbf{B}_{1:k}(\mathbf{x}) \mathbf{U}_{1:k}$ . For appropriately sized matrices  $\mathbf{P}, \mathbf{Q}, \mathbf{R}, \mathbf{S}$ , the Kronecker product satisfies  $(\mathbf{P} \otimes \mathbf{Q})(\mathbf{R} \otimes \mathbf{S}) = (\mathbf{PR} \otimes \mathbf{QS})$  and  $(\mathbf{P} \otimes \mathbf{Q})^{-1} = \mathbf{P}^{-1} \otimes \mathbf{Q}^{-1}$ . Thus, we can rewrite the mean as:

$$\begin{aligned} \text{vec}(\mathbf{M}_k(\mathbf{x})) &= \text{vec}(\mathbf{M}_0(\mathbf{x})) + \\ &\left( (\mathbf{B}_{1:k}^\top(\mathbf{x}) [\mathbf{B}_{1:k}^{1:k}]^{-1}) \otimes \mathbf{A} \mathbf{A}^{-1} \right) \text{vec}(\mathbf{X} - \mathbf{M}_{1:k} \mathbf{U}_{1:k}). \end{aligned} \quad (49)$$

Applying  $(\mathbf{P} \otimes \mathbf{Q}) \text{vec}(\mathbf{R}) = \text{vec}(\mathbf{QRP}^\top)$ , we get

$$\begin{aligned} \mathbf{M}_k(\mathbf{x}) &= \mathbf{M}_0(\mathbf{x}) + (\mathbf{X}_{1:k} - \mathbf{M}_{1:k} \mathbf{U}_{1:k}) [\mathbf{B}_{1:k}^{1:k}]^{-1} \mathbf{B}_{1:k}^\top(\mathbf{x}). \\ &= \mathbf{M}_0(\mathbf{x}) + (\mathbf{X}_{1:k} - \mathbf{M}_{1:k} \mathbf{U}_{1:k}) (\mathbf{U}_{1:k} \mathbf{B}_{1:k}(\mathbf{x}))^\dagger \end{aligned} \quad (50)$$

Similarly, the covariance can be rewritten as,

$$\begin{aligned} \mathbf{K}_k(\mathbf{x}, \mathbf{x}') &= (\mathbf{B}_0(\mathbf{x}, \mathbf{x}') - \mathbf{B}_{1:k}(\mathbf{x}) [\mathbf{B}_{1:k}^{1:k}]^{-1} \mathbf{B}_{1:k}^\top(\mathbf{x}')) \otimes \mathbf{A} \\ &= (\mathbf{B}_0(\mathbf{x}, \mathbf{x}') - \mathbf{B}_{1:k}(\mathbf{x}') \mathbf{U}_{1:k} (\mathbf{U}_{1:k} \mathbf{B}_{1:k}(\mathbf{x}))^\dagger) \otimes \mathbf{A}. \end{aligned} \quad (51)$$

Defining  $\mathbf{B}_k(\mathbf{x}, \mathbf{x}')$  such that  $\mathbf{K}_k(\mathbf{x}, \mathbf{x}) = \mathbf{B}_k(\mathbf{x}, \mathbf{x}') \otimes \mathbf{A}$ , we can write the posterior distribution of  $\text{vec}(F(\mathbf{x}))$  as  $\mathcal{GP}(\text{vec}(\mathbf{M}_k(\mathbf{x})), \mathbf{B}_k(\mathbf{x}, \mathbf{x}') \otimes \mathbf{A})$ .  $\square$

## APPENDIX C

## COREGIONALIZATION GAUSSIAN PROCESS

Here, we show how the Coregionalization model [71] can be applied to Gaussian process inference when the training data is available as a matrix vector product.

**Lemma 6.** Let  $\text{vec}(F(\mathbf{x})) \sim \mathcal{GP}(\text{vec}(\mathbf{M}_0(\mathbf{x})), \Sigma_{\kappa_0}(\mathbf{x}, \mathbf{x}'))$ , where  $\Sigma \in \mathbb{R}^{(1+m)n \times (1+m)n}$  is the covariance matrix of the

output dimensions, and  $\kappa_0(\mathbf{x}, \mathbf{x}')$  is the kernel function. Denote the kernel function evaluation over the training data as,

$$\begin{aligned} \mathbf{K}_{1:k}^{1:k} &\triangleq \begin{bmatrix} \kappa_0(\mathbf{x}_1, \mathbf{x}_1) & \dots & \kappa_0(\mathbf{x}_k, \mathbf{x}_1) \\ \vdots & & \vdots \\ \kappa_0(\mathbf{x}_k, \mathbf{x}_1) & \dots & \kappa_0(\mathbf{x}_k, \mathbf{x}_k) \end{bmatrix} \in \mathbb{R}^{k \times k} \\ \mathbf{K}_{1:k}(\mathbf{x}) &\triangleq [\kappa_0(\mathbf{x}_1, \mathbf{x}) \quad \dots \quad \kappa_0(\mathbf{x}_k, \mathbf{x})] \in \mathbb{R}^{1 \times k}. \end{aligned} \quad (52)$$

Let  $\mathbf{M}_{1:k}$  and  $\mathbf{U}_{1:k}$  be defined as in Proposition 3. Then, the posterior distribution of  $\text{vec}(F(\mathbf{x}))$ , given the training data  $(\mathbf{X}_{1:k}, \mathbf{X}_{1:k}, \mathbf{U}_{1:k})$ , is  $\mathcal{GP}(\text{vec}(\mathbf{M}_k(\mathbf{x})), \mathbf{K}_k(\mathbf{x}, \mathbf{x}'))$ , where

$$\begin{aligned} \text{vec}(\mathbf{M}_k(\mathbf{x})) &\triangleq \text{vec}(\mathbf{M}_0(\mathbf{x})) + \\ &\mathbf{K}_{1:k}(\mathbf{x}) [\mathbf{K}_{1:k}^{1:k}]^{-1} \text{vec}(\mathbf{X}_{1:k} - \mathbf{M}_{1:k} \mathbf{U}_{1:k}), \quad (53) \\ \mathbf{K}_k(\mathbf{x}, \mathbf{x}') &\triangleq \Sigma_{\kappa_0}(\mathbf{x}, \mathbf{x}') - \mathbf{K}_{1:k}(\mathbf{x}) [\mathbf{K}_{1:k}^{1:k}]^{-1} \mathbf{K}_{1:k}^\top(\mathbf{x}'), \end{aligned}$$

$\mathbf{K}_{1:k}^{1:k} \triangleq (\mathbf{U}_{1:k}^\top \otimes \mathbf{I}_n) (\mathbf{K}_{1:k}^{1:k} \otimes \Sigma) (\mathbf{U}_{1:k} \otimes \mathbf{I}_n) + \mathbf{I}_k \otimes \mathbf{S}$ , and  $\mathbf{K}_{1:k}(\mathbf{x}) \triangleq (\mathbf{K}_{1:k}(\mathbf{x}) \otimes \Sigma) (\mathbf{U}_{1:k} \otimes \mathbf{I}_n)$ .

*Proof.* Using  $\text{vec}(\mathbf{PQR}) = (\mathbf{R}^\top \otimes \mathbf{P}) \text{vec}(\mathbf{Q})$ , we can rewrite  $F(\mathbf{x}) \mathbf{u}$  as

$$F(\mathbf{x}) \mathbf{u} = \text{vec}(\mathbf{I}_n F(\mathbf{x}) \mathbf{u}) = (\mathbf{u}^\top \otimes \mathbf{I}_n) \text{vec}(F(\mathbf{x})). \quad (54)$$

Thus, the variance of  $F(\mathbf{x}) \mathbf{u}$  can be expressed in terms of the kernel  $\Sigma_{\kappa_0}(\mathbf{x}, \mathbf{x}')$ :

$$F(\mathbf{x}) \mathbf{u} \sim \mathcal{N}(\mathbf{M}_0(\mathbf{x}) \mathbf{u}, (\mathbf{u}^\top \otimes \mathbf{I}_n) \Sigma_{\kappa_0}(\mathbf{x}, \mathbf{x}') (\mathbf{u} \otimes \mathbf{I}_n)). \quad (55)$$

The training data is generated from  $\mathbf{x} = F(\mathbf{x}) \mathbf{u} + \mathbf{w}$  with  $\mathbf{w} \sim \mathcal{N}(\mathbf{0}_n, \mathbf{S})$  and is jointly Gaussian:

$$\text{vec}(\mathbf{X}_{1:k}) \sim \mathcal{N}(\text{vec}(\mathbf{M}_{1:k} \mathbf{U}_{1:k}), \mathbf{K}_{1:k}^{1:k}), \quad (56)$$

The covariance for a single point is given by,

$$\begin{aligned} \text{cov}(\text{vec}(F(\mathbf{x})), F(\mathbf{x}') \mathbf{u}) &= \text{cov}(\text{vec}(F(\mathbf{x})), (\mathbf{u}^\top \otimes \mathbf{I}_n) \text{vec}(F(\mathbf{x}')))) \\ &= \Sigma_{\kappa_0}(\mathbf{x}, \mathbf{x}') (\mathbf{u} \otimes \mathbf{I}_n). \end{aligned} \quad (57)$$

A similar expression for covariance can be obtained between the training data and the test data,  $\text{cov}(\text{vec}(F(\mathbf{x})), \mathbf{X}_{1:k}) = \mathbf{K}_{1:k}(\mathbf{x})$ . We can now write the joint distribution between the training and test data,

$$\begin{aligned} \begin{bmatrix} \text{vec}(\mathbf{X}_{1:k}) \\ \text{vec}(F(\mathbf{x})) \end{bmatrix} &\sim \mathcal{N} \left( \begin{bmatrix} \text{vec}(\mathbf{M}_{1:k} \mathbf{U}_{1:k}) \\ \mathbf{M}_0(\mathbf{x}) \end{bmatrix}, \right. \\ &\left. \begin{bmatrix} \mathbf{K}_{1:k}^{1:k} & \mathbf{K}_{1:k}^\top(\mathbf{x}') \\ \mathbf{K}_{1:k}(\mathbf{x}) & \Sigma_{\kappa_0}(\mathbf{x}, \mathbf{x}') \end{bmatrix} \right) \end{aligned} \quad (58)$$

Applying a Schur complement, we get the posterior distribution in (53).  $\square$

## APPENDIX D

## PROOF OF PROPOSITION 7

Recall the definition of  $\text{CBC}^{(r)}(\mathbf{x}, \mathbf{u})$ :

$$\begin{aligned} \text{CBC}^{(r)}(\mathbf{x}, \mathbf{u}) &= \mathcal{L}_f^{(r)} h(\mathbf{x}) + \mathcal{L}_g \mathcal{L}_f^{(r-1)} h(\mathbf{x}) \mathbf{u} + \mathbf{k}_\alpha^\top \eta(\mathbf{x}) \\ &= \mathcal{L}_f [\mathcal{L}_f^{(r-1)} h(\mathbf{x})] + \mathcal{L}_g [\mathcal{L}_f^{(r-1)} h(\mathbf{x})] \mathbf{u} + \mathbf{k}_\alpha^\top \eta(\mathbf{x}) \\ &= \nabla_{\mathbf{x}} [\mathcal{L}_f^{(r-1)} h(\mathbf{x})]^\top f(\mathbf{x}) + \nabla_{\mathbf{x}} [\mathcal{L}_f^{(r-1)} h(\mathbf{x})]^\top g(\mathbf{x}) \mathbf{u} + \mathbf{k}_\alpha^\top \eta(\mathbf{x}) \\ &= \nabla_{\mathbf{x}} [\mathcal{L}_f^{(r-1)} h(\mathbf{x})]^\top F(\mathbf{x}) \mathbf{u} + \mathbf{k}_\alpha^\top \eta(\mathbf{x}). \end{aligned}$$

Since,  $\mathbf{u} = [1, \mathbf{u}^\top]^\top$ , we can rewrite the above as

$$\text{CBC}^{(r)}(\mathbf{x}, \mathbf{u}) = \left( \nabla_{\mathbf{x}} \mathcal{L}_f^{(r-1)} h(\mathbf{x})^\top F(\mathbf{x}) + \begin{bmatrix} \mathbf{k}_\alpha^\top \eta(\mathbf{x}) \\ \mathbf{0}_m \end{bmatrix}^\top \right) \mathbf{u}$$

Using linearity of expectation, we see that  $\mathbb{E}[\text{CBC}^{(r)}(\mathbf{x}, \mathbf{u})]$  is linear in  $\mathbf{u}$ :

$$\begin{aligned} \mathbb{E}[\text{CBC}^{(r)}(\mathbf{x}, \mathbf{u})] &= \underbrace{\left( \mathbb{E}[F(\mathbf{x})^\top \nabla_{\mathbf{x}} \mathcal{L}_f^{(r-1)} h(\mathbf{x})] + \mathbb{E} \left[ \begin{bmatrix} \mathbf{k}_\alpha^\top \eta(\mathbf{x}) \\ \mathbf{0}_m \end{bmatrix} \right] \right)^\top}_{\mathbf{e}^{(r)}(\mathbf{x})} \mathbf{u}. \end{aligned} \quad (59)$$

Also, applying  $\text{Var}(\mathbf{x}^\top \mathbf{u}) = \text{Var}(\mathbf{u}^\top \mathbf{x}) = \mathbf{u}^\top \text{Var}(\mathbf{x}) \mathbf{u}$  to  $\text{CBC}^{(r)}(\mathbf{x}, \mathbf{u})$ , we get:

$$\begin{aligned} \text{Var}[\text{CBC}^{(r)}(\mathbf{x}, \mathbf{u})] &= \mathbf{u}^\top \underbrace{\text{Var} \left[ \nabla_{\mathbf{x}} \mathcal{L}_f^{(r-1)} h(\mathbf{x})^\top F(\mathbf{x}) + \begin{bmatrix} \mathbf{k}_\alpha^\top \eta(\mathbf{x}) \\ \mathbf{0}_m \end{bmatrix}^\top \right]}_{\mathbf{V}^{(r)}(\mathbf{x}) \mathbf{V}^{(r)}(\mathbf{x})^\top} \mathbf{u}. \quad \square \end{aligned} \quad (60)$$

#### APPENDIX E PROOF OF PROPOSITION 8

Unlike CBC for relative degree one, the distribution of  $\text{CBC}^{(r)}$  is not a Gaussian Process for  $r \geq 2$ . Hence, instead of computing the probability distribution analytically, we use Cantelli's inequality to bound the mean and variance of  $\text{CBC}_k^{(r)}$ . For any scalar  $\lambda > 0$ , we have

$$\begin{aligned} \mathbb{P}(\text{CBC}_k^{(r)} \geq \mathbb{E}[\text{CBC}_k^{(r)}] - \lambda \mid \mathbf{x}_k, \mathbf{u}_k) &\geq \\ 1 - \frac{\text{Var}[\text{CBC}_k^{(r)}]}{\text{Var}[\text{CBC}_k^{(r)}] + \lambda^2}. \end{aligned} \quad (61)$$

Since we want the probability to be greater than  $\tilde{p}_k$ , we ensure its lower bound is greater than  $\tilde{p}_k$ , i.e.,

$$1 - \frac{\text{Var}[\text{CBC}_k^{(r)}]}{\text{Var}[\text{CBC}_k^{(r)}] + \lambda^2} \geq \tilde{p}_k. \quad (62)$$

The terms can be rearranged into,

$$\begin{aligned} (1 - \tilde{p}_k)(\text{Var}[\text{CBC}_k^{(r)}] + \lambda^2) &\geq \text{Var}[\text{CBC}_k^{(r)}] \\ \lambda &\geq \sqrt{\frac{\tilde{p}_k}{1 - \tilde{p}_k} \text{Var}[\text{CBC}_k^{(r)}]}. \end{aligned} \quad (63)$$

For some desired margin,  $\mathbb{E}[\text{CBC}_k^{(r)}] \geq \zeta$ , we can substitute  $\lambda = (\mathbb{E}[\text{CBC}_k^{(r)}] - \zeta) > 0$  in (63), so that:

$$\begin{aligned} \mathbb{E}[\text{CBC}_k^{(r)}] - \zeta &> \sqrt{\frac{\tilde{p}_k}{1 - \tilde{p}_k} \text{Var}[\text{CBC}_k^{(r)}]} \\ \implies \mathbb{P}(\text{CBC}_k^{(r)} \geq \zeta \mid \mathbf{x}_k, \mathbf{u}_k) &\geq \tilde{p}_k \end{aligned} \quad (64)$$

Using the tighter constraint above in (26) and the explicit expressions in (59) and (60) for the mean and variance of  $\text{CBC}_k^{(r)}$ , we get:

$$\pi(\mathbf{x}_k) \in \arg \min_{\mathbf{u}_k \in \mathcal{U}} \|\mathbf{R}(\mathbf{x}_k) \mathbf{u}_k\|_2 \quad (65)$$

$$\text{s.t. } \mathbf{e}_k^{(r)}(\mathbf{x}_k)^\top \mathbf{u}_k - \zeta - c^{(r)}(\tilde{p}_k) \left\| \mathbf{V}_k^{(r)}(\mathbf{x}_k) \mathbf{u}_k \right\|_2 \geq 0,$$

where  $c^{(r)}(\tilde{p}_k) = \sqrt{\frac{\tilde{p}_k}{1 - \tilde{p}_k}}$ . To ensure that (65) is a standard SOCP, we convert the objective into a SOCP constraint by introducing an auxiliary variable  $y$ , leading to (30).  $\square$

#### APPENDIX F PROOF OF LEMMA 2

Recall the following result about the mean and cumulants of a quadratic form of Gaussian random vectors.

**Lemma 7** ([97, p. 55]). *Let  $\mathbf{x}$  be a Gaussian random vector with mean  $\bar{\mathbf{x}}$  and covariance matrix  $\Sigma$ . Let  $\Lambda$  be a symmetric matrix and consider the random variable  $\mathbf{x}^\top \Lambda \mathbf{x}$ . The mean of  $\mathbf{x}^\top \Lambda \mathbf{x}$  is*

$$\mathbb{E}[\mathbf{x}^\top \Lambda \mathbf{x}] = \bar{\mathbf{x}}^\top \Lambda \bar{\mathbf{x}} + \text{tr}(\Lambda \Sigma).$$

The  $r$ th cumulant of  $\mathbf{x}^\top \Lambda \mathbf{x}$  is:

$$\mathcal{K}_r(\mathbf{x}^\top \Lambda \mathbf{x}) = 2^{r-1} (r-1)! [\text{tr}(\Lambda \Sigma)^r + r \bar{\mathbf{x}}^\top \Lambda (\Sigma \Lambda)^{r-1} \bar{\mathbf{x}}].$$

The variance of  $\mathbf{x}^\top \Lambda \mathbf{x}$  is the second cumulant:

$$\text{Var}[\mathbf{x}^\top \Lambda \mathbf{x}] = \mathcal{K}_2(\mathbf{x}^\top \Lambda \mathbf{x}) = 2 \text{tr}(\Lambda \Sigma)^2 + 4 \bar{\mathbf{x}}^\top \Lambda \Sigma \Lambda \bar{\mathbf{x}}.$$

The covariance between  $\mathbf{x}$  and  $\mathbf{x}^\top \Lambda \mathbf{x}$  is:

$$\text{cov}(\mathbf{x}, \mathbf{x}^\top \Lambda \mathbf{x}) = 2 \Sigma \Lambda \bar{\mathbf{x}}$$

Returning to the proof of Lemma 2, consider the three Gaussian random vectors  $\mathbf{x}$ ,  $\mathbf{y}$ , and  $\mathbf{z}$ . Note that  $\mathbf{x}^\top \mathbf{y}$  can be written as a quadratic form:

$$\mathbf{x}^\top \mathbf{y} = \frac{1}{2} \begin{bmatrix} \mathbf{x}^\top & \mathbf{y}^\top & \mathbf{z}^\top \end{bmatrix} \begin{bmatrix} 0 & \mathbf{I} & 0 \\ \mathbf{I} & 0 & 0 \\ 0 & 0 & 0 \end{bmatrix} \begin{bmatrix} \mathbf{x} \\ \mathbf{y} \\ \mathbf{z} \end{bmatrix}. \quad (66)$$

Applying Lemma 7 to (66), shows that:

$$\begin{aligned} \mathbb{E}[\mathbf{x}^\top \mathbf{y}] &= \bar{\mathbf{x}}^\top \bar{\mathbf{y}} + \frac{1}{2} \text{tr}(\text{cov}(\mathbf{x}, \mathbf{y}) + \text{cov}(\mathbf{y}, \mathbf{x})) \\ \text{Var}[\mathbf{x}^\top \mathbf{y}] &= \frac{1}{2} \text{tr}(\text{cov}(\mathbf{x}, \mathbf{y}) + \text{cov}(\mathbf{y}, \mathbf{x}))^2 + \bar{\mathbf{y}}^\top \text{Var}[\mathbf{x}] \bar{\mathbf{y}} \\ &\quad + \bar{\mathbf{x}}^\top \text{Var}[\mathbf{y}] \bar{\mathbf{x}} + \bar{\mathbf{y}}^\top \text{cov}(\mathbf{x}, \mathbf{y}) \bar{\mathbf{x}} + \bar{\mathbf{x}}^\top \text{cov}(\mathbf{y}, \mathbf{x}) \bar{\mathbf{y}} \\ \begin{bmatrix} \text{cov}(\mathbf{x}, \mathbf{x}^\top \mathbf{y}) \\ \text{cov}(\mathbf{y}, \mathbf{x}^\top \mathbf{y}) \\ \text{cov}(\mathbf{z}, \mathbf{x}^\top \mathbf{y}) \end{bmatrix} &= \text{cov} \left( \begin{bmatrix} \mathbf{x} \\ \mathbf{y} \\ \mathbf{z} \end{bmatrix}, \mathbf{x}^\top \mathbf{y} \right) \\ &= 2 \begin{bmatrix} \text{Var}[\mathbf{x}] & \text{cov}(\mathbf{x}, \mathbf{y}) & \text{cov}(\mathbf{x}, \mathbf{z}) \\ \text{cov}(\mathbf{y}, \mathbf{x}) & \text{Var}[\mathbf{y}] & \text{cov}(\mathbf{y}, \mathbf{z}) \\ \text{cov}(\mathbf{z}, \mathbf{x}) & \text{cov}(\mathbf{z}, \mathbf{y}) & \text{Var}[\mathbf{z}] \end{bmatrix} \frac{1}{2} \begin{bmatrix} \bar{\mathbf{y}} \\ \bar{\mathbf{x}} \\ \mathbf{0} \end{bmatrix} \quad \square \end{aligned}$$